Received: 20 September 2019 | Revised: 23 November 2019 | Accepted: 8 December 2019

DOI: 10.1002/ardp.201900267

DPhG ARCH PHARM
Archiv der Pharmazie

FULL PAPER

rac- and *meso*-Cyclohexanoids: Their α-, β-glycosidases, antibacterial, antifungal activities, and molecular docking studies

Emel Karakılıç[1] | Şule Baran[2] | Hatice Öğütçü[3] | Atilla Akdemir[4] | Arif Baran[1]

[1]Department of Chemistry, Sakarya University, Sakarya, Turkey

[2]Department of Biology, Sakarya University, Sakarya, Turkey

[3]Department of Biology, Ahievran University, Kırşehir, Turkey

[4]Department of Pharmacology, Bezmialem Vakif University, Istanbul, Turkey

Correspondence
Arif Baran, Department of Chemistry, Sakarya University, 54187 Sakarya, Turkey.
Email: abaran@sakarya.edu.tr

Funding information
The Scientific and Technological Research Council of Turkey (TUBITAK), Grant/Award Number: KBAG-217Z043; Unit of Scientific Research Projects of Sakarya University, Grant/Award Numbers: 2017-02-04-027, 2018-01-06-153

Abstract

An efficient and versatile synthesis method has been postulated for hydroxymethylated *rac*- and *meso*-cyclohexanoid derivatives. The synthesis of these stereoisomers was achieved easily with traditional methods using hexahydroisobenzofuran **6**, prepared from commercially available *cis*-hydrophthalic anhydride. The study, involving diastereoselective epoxidation and *cis*-hydroxylation, was conducted to obtain epoxy-, *cis*-, and *trans*-diol-furans **7**, **8**, and **9**. After sulfamic acid-catalyzed ring-opening reaction of the epoxide and furan rings, *rac*- and *meso*-tetraacetates **14**, **15**, and **16** were afforded. Hydrolysis of acetate groups with ammonia in absolute methanol yielded the desired tetrols *rac*-**17**, *meso*-**18**, and *meso*-**19**. All structures, after purification by chromatographic methods and elucidation by spectral techniques, were screened against α- and β-glucosidases. Compounds **7**, **8**, **10**, **17**, **18**, and **19** were also evaluated for their antibacterial and antifungal activity against some selected synthesized compounds with varying degrees of inhibitory effects on the growth of different pathogenic microorganisms by the well-diffusion method. In addition, *Saccharomyces cerevisiae* α-glucosidase molecular modeling studies were performed for all *rac*- and *meso*-compounds **7**, **8**, **10**, **17**, **18**, and **19**.

KEYWORDS
antifungal activity, antimicrobial activity, assay, inhibitors

1 | INTRODUCTION

Throughout history, chemical substances isolated from animals, plants, and microorganisms have been used for treating many diseases. In particular, cyclohexanoid polyols and their derivatives have always been rich resources for the discovery and development of new drugs.[1] Natural products are generally hydrocarbons, that is, organic compounds, containing functional groups such as alcohols, ketones, aldehydes, carboxylic acids, and ethers, that may contain heteroatoms (such as N and O).[2] Moreover, sugar units,[3] terpenoids, flavonoids, steroids, alkaloids, iridoids, stilbenoids, and phenylpropanoids constitute important classes of natural products containing heteroatoms (O and N) in their constructions.[4]

Glycosidase inhibitors (sugars or pseudosugars, containing −O atoms) prepared naturally or synthetically can be divided into classes such as cyclohexanetetrols (**1** and **2**), cyclohexanepentols (**3**), and cyclohexanehexols (**4** and **5**), and their hydroxymethyl-containing derivatives (Figure 1).

Cyclohexanoid structures having polyhydroxylated nuclei are found in many biologically important molecules and natural products. Their promising biological activity profiles were reported, ranging from glycosidase inhibitors to antidiabetes and anticancer agents.[5,6]

Furthermore, there are covalent-type glycosidase inhibitors, including naturally occurring carbohydrates like acarbose and nojirimycin, as well as hydroxy- and amino-substituted bioactive aminoglicosides.[7] The nuclei of these inhibitors are involved in many

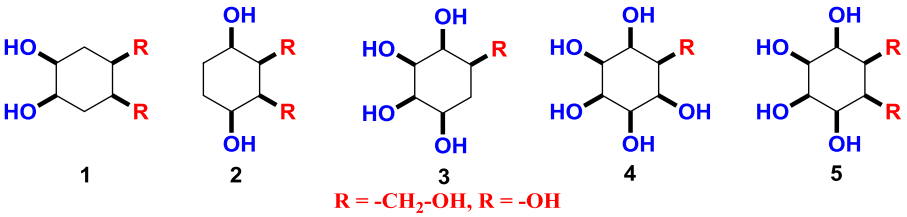

FIGURE 1 Polyhydroxy cyclohexanoids

biological processes, from cellular communication to inhibition of glucosidase.[8,9]

Glycosidase inhibitors are known to be antidiabetic, anti-influenza,[10,11] antimicrobial, herbicidal,[12] antitumor, antibacterial,[13a] antileukemia,[14] anti-HIV,[15] and antihypergens,[16] and they are also responsible for intercellular recognition, signal transduction, and cellular development.[17]

As a result, cyclohexene or cyclohexane polyols (conduritols, quercitols, and inositols) and their derivatives have the potential to be key intermediates in the preparation of certain natural products and biologically important molecules.[18] Thus, we synthesized cyclohexanetetrol stereoisomers containing hydroxymethyl cyclohexanoid nuclei with a series of stereospecific reactions by readily accessible anhydrides. All intermediate and final products obtained were separated and purified by using traditional chromatographic techniques, and all the purified products were clarified by spectroscopic methods and were screened against α- and β-glucosidases using acarbose as a positive control. Newly synthesized compounds (*rac*-**10**, -**17**, and *meso*-**7**, -**8**, -**18**, -**19**) were investigated for their antimicrobial activity against pathogenic strains (Gram[−] and Gram[+] bacteria and yeast): *Staphylococcus aureus*, *Staphylococcus epidermidis*, *Pseudomonas putida*, *Escherichia coli*, *Salmonella typhi* H, *Micrococcus luteus*, *Bacillus cereus*,[19] *Klebsiella pneumoniae*, *Proteus vulgaris*, *Enterobacter aerogenes*, and *Candida albicans*. Molecular modeling studies were performed for the same molecules **7**, **8**, **10**, **17**, **18**, and **19**, as well as maltose, obtained from the crystal structure active site, and they were docked into the active site of *Saccharomyces cerevisiae* α-glucosidase. *meso*-Compounds **18** and **19** showed inhibition of *S. cerevisiae* α-glucosidase in the micromolar range, whereas the structural analogue *rac*-compound **17** and the other compounds did not show any significant inhibition. Moreover, *rac*- and *meso*-compounds **17**–**19** have the potential to form many more hydrogen bonds with the active site of *S. cerevisiae* α-glucosidase.

2 | RESULTS AND DISCUSSION

2.1 | Synthesis and characterization

Starting from dihydroisobenzofuran **6**, cyclohexane-*cis*-diols containing hydrofuran cyclohexane nuclei were synthesized after *cis*-hydroxylation and hydrolysis reactions. In the reaction, the double bond in dihydroisobenzofuran **6** was first oxidized with *m*-chloroperoxybenzoic acid (*m*-CPBA) in dichloromethane (DCM) and OsO_4/NMO couple in water and acetone. After hydrolysis and pH adjustment, epoxy **9** (81%) and a mixture of *meso*-diols **7** (63.7%) and **8** (29.7%) were afforded (Scheme 1).[20,21]

After separation of the diol mixture by column chromatography on silica gel, two stereoisomers were afforded successfully by changing the solution ratio. The reaction occurred at the free face to give first isomer *meso*-**7** as the major product, as shown in Scheme 2 (63.7% yield).

The scaffolds were determined based on the nuclear magnetic resonance (NMR) spectra and all coupling constants were reviewed for *meso*-**7** and -**8**. For construction **7**, the resonance signal between H_1 and H_2 protons and a proton of H_{5a} or $H_{5a'}$ was measured as a multiplet at 3.85 ppm, and the interaction between neighboring group protons, H_1 and $H_6H_{6'}$ or H_2 and $H_3H_{3'}$, could not be determined. Similarly, for construction **8**, the resonance signal between the protons H_1, H_2, and H_{5a}, $H_{5a'}$ or H_{4a}, $H_{4a'}$ was measured as a multiplet at 3.76 ppm. Again, the interaction between neighboring group protons, H_1 and $H_6H_{6'}$ or H_2 and $H_3H_{3'}$, could not be determined. To see the coupling constants in more detail for both constructions *meso*-**7** and -**8**, we changed the NMR deuterium solution ($CDCl_3$) and used *d*-benzene, *d*-methanol, *d*-acetone, and so on, but the configurations could not be determined exactly. Therefore, we prepared and verified construction *meso*-**7** by single-crystal X-ray analysis (Figure 2).

Furthermore, for the synthesis of cyclohexane-*trans*-diols, dihydroisobenzofuran, containing hydrofuran cyclohexane core **6**, was

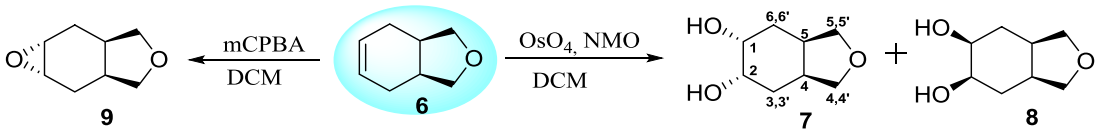

SCHEME 1 Synthesis of compounds **7** and **8**. DCM, dichloromethane; *m*-CPBA, *m*-chloroperoxybenzoic acid

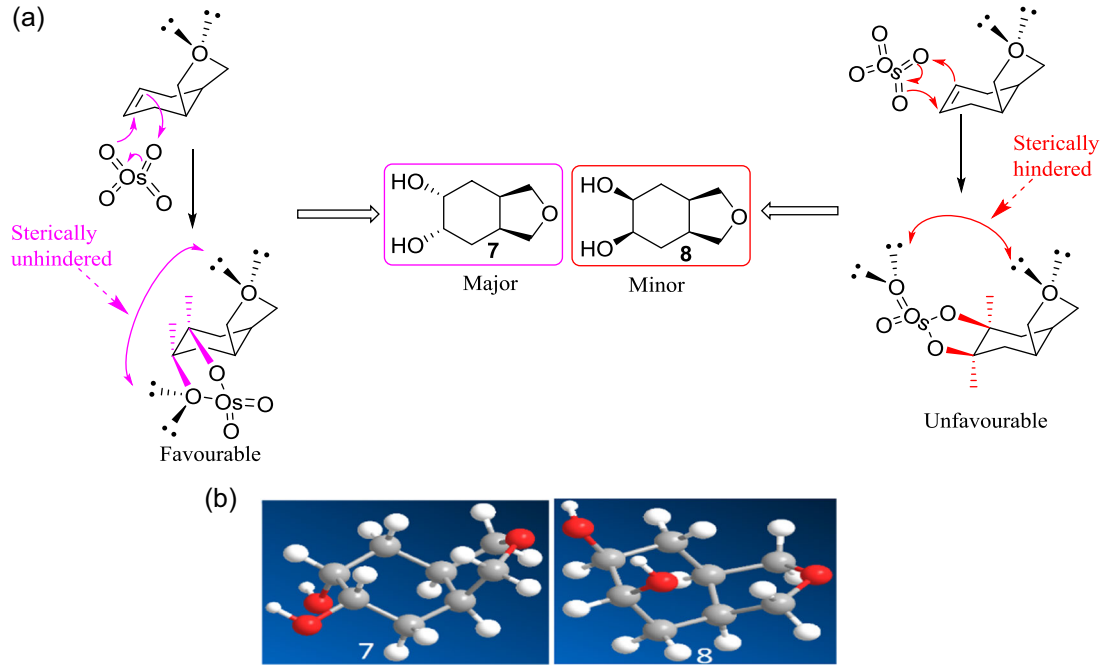

SCHEME 2 (a) Two-dimensional schematic diagram for stereoselectivity of *meso*-**7** and -**8** structures. (b) Three-dimensional schematic diagrams for stereoselectivity of *rac*-**7** and -**8** with calculating MM2 energy

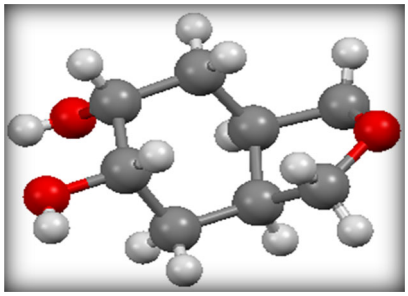

FIGURE 2 Single crystal of **7**

subjected to epoxidation reactions, and the epoxy *meso*-**9** was yielded as the sole product stereospecifically.

During the epoxidation reaction, the sterically hindered product was not afforded as in Scheme 3, whereas the unhindered product **9** was afforded quantitatively. The most prominent aspect of the epoxy-furan core is the carbon resonance signals in the ^{13}C-NMR spectra; four carbon signals exhibit a symmetric structure clearly showing a *trans* epoxy–hydrofuran couple (Scheme 2). In the proton NMR spectra, the resonance signal of the methylenic protons of the cyclohexane ring ($H_{33'}$ and $H_{66'}$ protons) at 1.72 and 1.19 ppm appears as an AB system with coupling constants of

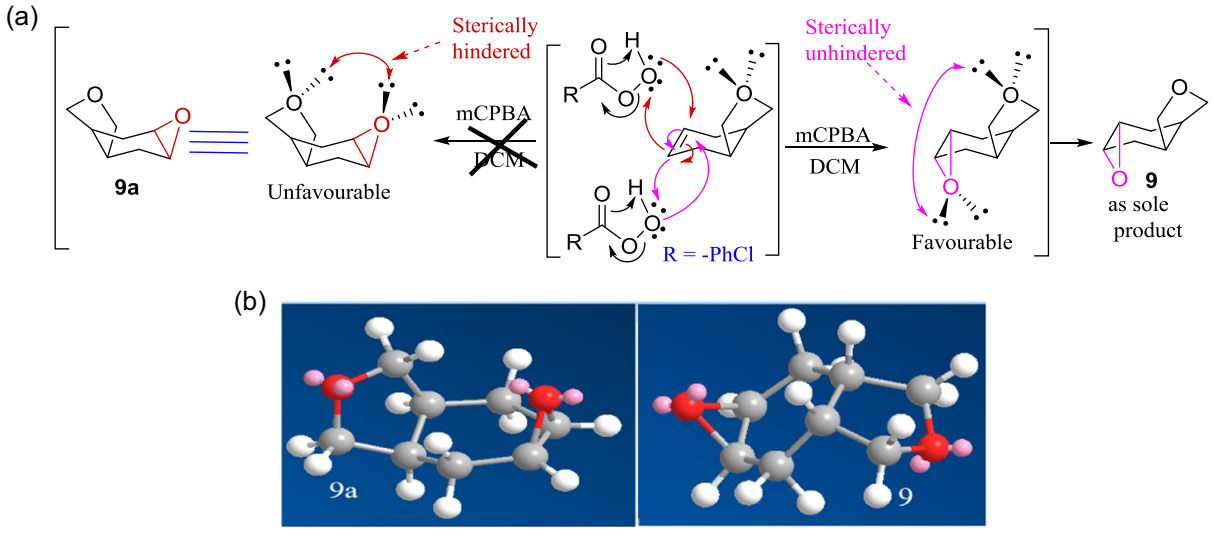

SCHEME 3 (a) Two-dimensional schematic diagram for stereoselectivity of compounds **9** and **9a**. (b) Three-dimensional schematic diagrams for stereoselectivity of meso-**9** and -**9a** with calculating MM2 energy. DCM, dichloromethane; *m*-CPBA, *m*-chloroperoxybenzoic acid

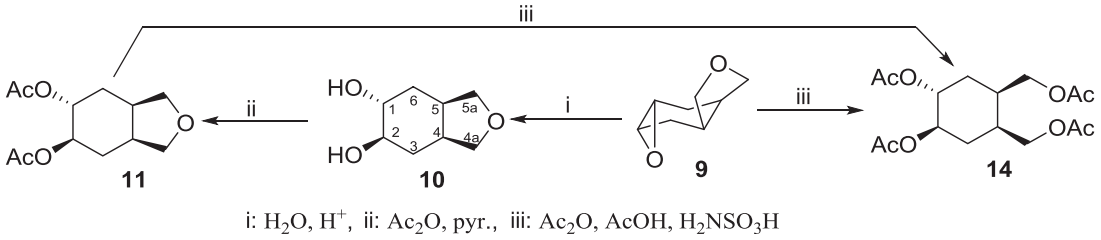

SCHEME 4 Synthesis of compound **14**

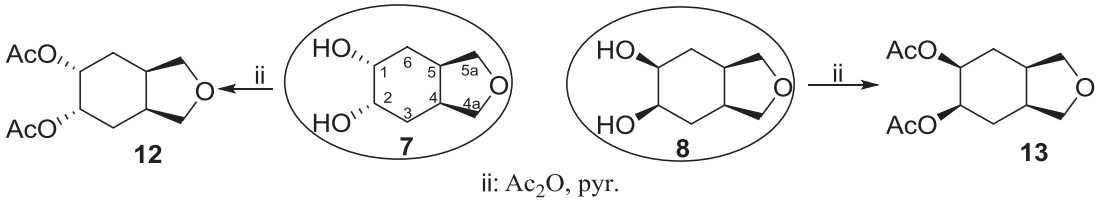

SCHEME 5 Synthesis of compound **13**

$J_{65(6'5)}$ or $_{34(3'4)}$ = 15.8 Hz, $J_{56'}$ or $_{33'}$ = 6.1 Hz and $J_{34(3'4)}$ or $_{65(6'5)}$ = 15.5 Hz, $J_{6'6}$ or $_{33'}$ = 6.1 Hz. The epoxy bound protons H-1 and H-2 resonate as broad singlets at 2.64 ppm. As a result, the correlation between H-1/H-2 and H-3/H-6 does not support the *cis*- or *trans*-configuration of the scaffold clearly because there is no interaction between methylene and epoxy protons. Therefore, we turned our attention to selective ring-opening of *meso*-epoxide **9**, and it was cleaved with the H_2O/H_2SO_4 couple to give *rac-trans*-diol **10** without any by-product or another stereoisomer, after purification and elaborative NMR results (Scheme 4). The reason we opened the epoxide with the H_2O/H_2SO_4 couple is that by-products do not occur during the opening of the epoxy ring.

On the contrary, it was determined that when Ac_2O and AcOH were used in the presence of a catalyst (H_2NSO_3),[13b,c] the epoxy and hydrofuran rings were opened, giving tetraacetate **14** directly without any by-product. Thus, examining the ^{1}H-NMR spectra for *rac*-diol **10**, the methylenic and quaternary protons (3,6,4,4a,5,5a) having different contours show that the structure can be *trans*. For the exact configuration, *rac*-structure **10** was submitted to an acetylation reaction using acetic anhydride in pyridine at room temperature, and, after purification, diacetate **11** was isolated as the sole product. Similar to scaffold **11**, other stereoisomers *meso*-**7** and -**8** were acetylated by the same procedure to give *meso*-**12** and -**13** quantitatively (Scheme 5).

Analysis of the NMR spectra for H-1 and H-2 protons at 5.01 and 4.87 ppm for scaffold **11** exhibits an AB system with the coupling constant $J_{12} = J_{21}$ = 11.0 Hz in *trans*-configuration. On the contrary, H-1 and H-2 protons at 5.12 ppm for symmetrical scaffold **12** exhibit the coupling constant $J_{12} = J_{21}$ = 2.9 Hz in the *cis* configuration, and for the other symmetrical scaffold **13**, J_{12} and/or J_{21} exhibit a multiplet at 5.09–5.05 ppm. All coupling constants for scaffolds **11–13** are summarized in Table 1.

After the characterization of diacetates **11–13**, the ring-opening of the tetrahydrofuran caught our attention. In the acetolysis of the tetrahydrofuran ring, sulfamic acid[13b,c] was used for efficient catalysis, using acetic anhydrite and acetic acid as reagent at the reflux temperature for the desired tetraacetates **14–16**. The nonsymmetrical construct **14** characterized by the ^{1}H-NMR and ^{13}C-NMR spectra exhibited that the configuration of the tetraacetates did not change during the ring-opening of tetrahydrofuran (Scheme 6) because the J_1 and J_2 coupling constants for *rac*-structures **11** and **14** were comparable. Whereas the H-1 proton for molecule **11** was resonating as ddd (J = 13.7, 11.0, 5.0 Hz) at 5.01 ppm, the H-2 proton was resonant as ddd (J = 11.0, 8.8, 4.4 Hz) at 4.87 ppm. This result shows that $J_{12} = J_{21}$ = 11.0 Hz and is *trans*. To obtain the *rac*-**14** structure, the tetrahydrofuran ring in the *rac*-**11** structure was opened with Ac_2O/AcOH using H_2NSO_3H as a catalyst. To elucidate the configuration with ^{1}H-NMR spectra, H-1 and H-2 were resonated at 4.98 and 4.88 ppm,

TABLE 1 ^{1}H (300 MHz)- and ^{13}C (75 MHz)-NMR (nuclear magnetic resonance) spectroscopic data of **11–13** in $CDCl_3$

Compounds	J_1 (Hz)	J_2 (Hz)	J_4 (Hz)	J_5 (Hz)	J_{44a} (Hz)	J_{55a} (Hz)	$J_{33'}$ (Hz)	$J_{66'}$ (Hz)
rac-**11**	13.7, 11.0, 5.0 ddd	15.2, 11.0, 4.4 ddd	7.6, 5.9, 2.1 dtd	14.9, 9.7, 5.9 ddd	9.1 *t* 8.2, 2.1 dd	8.5 *t* 8.5, 5.3 dd	13.2, 10.9 dt	14.3, 10.0, 5.9 ddd
meso-**12**	6.5, 2.9 dd (H_1 and H_2)		14.5, 10.5, 6.5 ddd (H_4 and H_5)		8.2, 6.8 dd ($H_{4a4a'}$ and $H_{5a5a'}$)		14.4, 5.9, 2.0 dtd ($H_{3a3a'}$ and $H_{6a6a'}$)	
meso-**13**	*m* (H_1 and H_2)		*m* (H_4 and H_5)		*m* ($H_{4a4a'}$ and $H_{5a5a'}$)		*m* ($H_{3a3a'}$ and $H_{6a6a'}$)	

SCHEME 6 Synthesis of compounds **17–19**

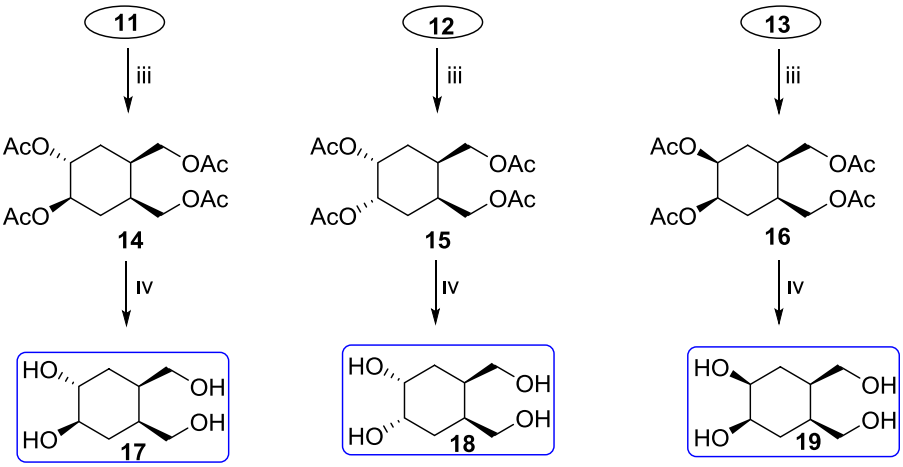

iii: Ac_2O, AcOH, H_2NSO_3H, IV: $NH_{3(g)}$, MeOH

giving ddd (J = 10.2, 8.6, 4.4 Hz) and dt (J = 8.6, 4.7 Hz), respectively. The coupling constants for the *rac*-**11** structure, $J_{12} = J_{21}$ = 11.0 Hz, and for the *rac*-**14** structure, $J_{12} = J_{21}$ = 8.6 Hz, indicate that the configuration of the structure is unchanged and *trans*.

To confirm the absolute configuration for *meso*-**15** and -**16** compounds, we first determined *cis* protons for J_{12} and J_{21} coupling constants as in *rac*-**14** compound, and overlapping protons H-1 and H-2 for two constructions at 5.12 and 5.05 ppm appeared as multiplets. Moreover, the other quaternary protons H-4 and H-5 gave multiplets for each structure at 2.35–2.05 and 2.21–2.09 ppm and the other vinylic protons H-3 and H-6 appeared as multiplets for the two structures as well. Finally, to obtain the target molecules, **14–16** were dissolved in methanol and ammonia was passed through the reaction medium to give the *rac*- and *meso*-tetrols **17–19** with yields of 91% for the **17**, 92% for the **18**, and 88% for the **19** separately after removal of water and acetamide.

2.2 | α-Glucosidase inhibition studies

The inhibitory activities of *rac*- and *meso*-diol-hydrofuran and tetrol compounds **7**, **8**, **10**, **17**, **18**, and **19** were screened against α-glycosidase. The results are summarized in Table 2. Though compounds *meso*-**18** and -**19** were found to be potent inhibitors of α-glycosidase with inhibition of 77.6 ± 1.59% for 180-μM concentration (IC_{50} = 91.67 μM) and 50 ± 4.39% for 180-μM concentration (IC_{50} = 527.39 μM), respectively, the other compounds showed weak inhibition toward α-glycosidase. The *rac*-tetrol **17** and *meso*-hydrofuran **8** showed moderate inhibition between 10 and 180 μM concentration. Although the *rac*-epoxy-hydrofuran **10** showed no activity after 40-μM concentration, the *meso*-hydrofuran **7** showed approximately 7–8 μM activity after 40-μM concentration and inhibition decreased with increasing concentration. Therefore, it can be said that *meso*-hydrofuran **7** shows no inhibition against α-glucosidase at concentrations greater than 40 μM (Figure 3).

According to the current work, when the α-glycosidase inhibition % for the tested *rac*- and *meso*-compounds **7**, **8**, **10**, **17**, **18**, **19**, and acarbose was compared between 10 and 180 μM concentration, acarbose exhibited the best activity at the corresponding concentrations. We can also say that the glucosidase inhibition %—concentration plot shows a proportional increase in the *rac*-**17**, *meso*-**18** and -**19** compounds. However, though the diol-furan compounds *rac*-**10** and *meso*-**8** appear to be stable, inhibition by *meso*-compound **7** appears to decrease after a certain concentration (Figure 3). The results are best demonstrated in the α-glucosidase inhibition%–concentration of compound graph (Figure 4).

TABLE 2 Inhibition of α-glucosidase by *rac*- and *meso*-diol-hydrofuran and tetrol compounds **8**, **10**, **17**, **18**, **19**, and acarbose

α-Glucosidase inhibition (%)[a]								
Compounds	**10 μM**	**20 μM**	**40 μM**	**60 μM**	**80 μM**	**1,120 μM**	**180 μM**	**IC_{50} (μM)[b]**
meso-**8**	6.54 ± 0.77	6.80 ± 1	7.71 ± 0.32	9.05 ± 0.51	11.07 ± 0.56	16.31 ± 053	17.59 ± 1.5	ND
rac-**10**	6.20 ± 2.04	9.38 ± 6.51	9.94 ± 5.34	–	–	–	–	ND
rac-**17**	25.8 ± 1.92	27.8 ± 2.83	29.31 ± 1.16	30.3 ± 0.54	33.24 ± 1.63	35.6 ± 1.16	40.8 ± 3.21	ND
meso-**18**	17.75 ± 7.16	23.63 ± 0.62	25.89 ± 0.64	33.1 ± 2.18	42.5 ± 6.22	52.5 ± 4.93	77.6 ± 1.59	91.67
meso-**19**	19.9 ± 2.69	21.68 ± 0.33	23.42 ± 0.34	25.78 ± 1.92	29.16 ± 0.26	34.99 ± 0.54	50 ± 4.39	527.39
Acarbose[c]	22.82 ± 1.44	30 ± 3.1	33 ± 1.5	46 ± 3.2	60 ± 0.71	68 ± 1.3	78 ± 0.05	52.16

Abbreviation: ND, not determined.

[a]Concentration required for 50% inhibition of the enzyme activity under the assay conditions.

[b]Four experiments were performed for all compounds in each experiment triplicated.

[c]Positive control.

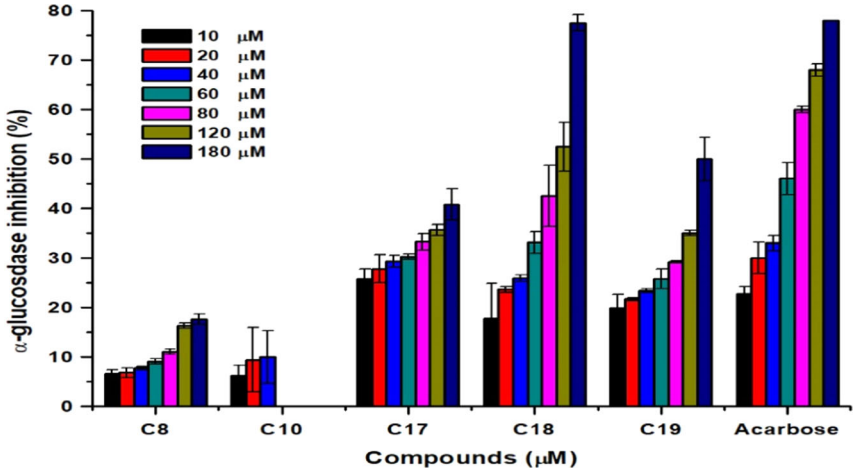

FIGURE 3 α-Glucosidase inhibition % for (10–180 µM) test compounds and acarbose control. Control of α-glucosidase inhibition % compared to acarbose concentration of C8 (**8**), C10 (**10**), C17 (**17**), C18 (**18**), and C19 (**19**), compounds. Mean values ± standard deviation are shown for triplicate experiments

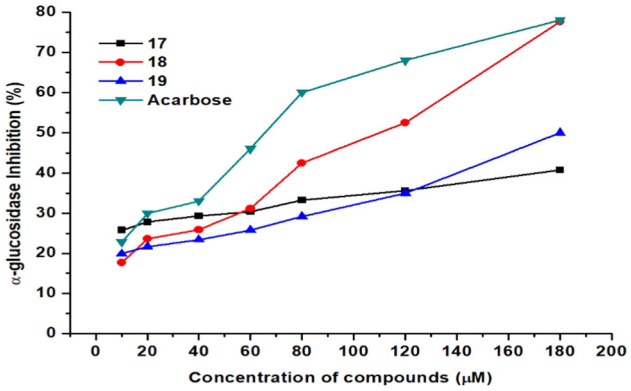

FIGURE 4 Inhibition % of α-glucosidase at different concentrations against acarbose and compounds **17–19**. The compounds were tested with concentrations ranging from 10 to 180 µM. Results are the means ± standard deviation of three replicates of each group

2.3 | β-Glucosidase inhibition studies

The inhibitory effects of the *rac*- and *meso*-target molecules **7**, **8**, **10**, **17**, **18**, and **19** were evaluated for β-glucosidase inhibition using acarbose as a positive control. The β-glucosidase inhibitory assay and its results are summarized in Table 3. The *meso*-tetrol **19** shows increased inhibition at stable concentrations, whereas other compounds show reduced inhibition after a certain concentration against acarbose.

The best inhibition activity was observed in *meso*-furan diol **7** with 51.09 ± 2.28% inhibition at 10 to 80 µM concentration (IC_{50} = 164.98 µM) compared to acarbose, whereas low β-glucosidase inhibition activity up to 40 µM was exhibited for *rac*-**10**, and *meso*-**17** compounds. And, it can be said that *meso*-hydrofuran **8** shows no inhibition against β-glucosidase at concentrations >40 µM. Furthermore, tetrol **18** showed moderate β-glucosidase inhibition activity up to 80 µM, whereas regular β-glucosidase inhibition activity among these was exhibited for *meso*-tetrol **19** with inhibition of 40.12 ± 0.78 for up to 180 µM. The results are exhibited in the β-glucosidase inhibition %–compound concentration (µM) plot (Figure 5).

According to the β-glucosidase inhibition (%)–concentration of compounds (µM) graph, all compounds except *meso*-tetrol **19** resulted in an increase or decrease in certain concentrations (Figure 6). However, *rac*-compounds **10** and **17** showed inhibition of about 36–37 µM and 7–8 µM, respectively, after 40 µM concentration. This indicates that the compounds are inactive after a certain concentration. Moreover, the inhibition activity of all compounds is shown in the β-glucosidase % inhibition–concentration of compounds (µM) graph in comparison with acarbose.

TABLE 3 Inhibition of β-glucosidase by *rac*- and *meso*-compounds **7**, **10**, **18**, **19**, and acarbose

β-Glucosidase inhibition (%)[a]								
Compounds	**10 µM**	**20 µM**	**40 µM**	**60 µM**	**80 µM**	**1,120 µM**	**180 µM**	**IC_{50} (µM)[b]**
meso-**7**	35.52 ± 0.91	41.12 ± 0.55	43.79 ± 1.09	47.57 ± 0.56	51.09 ± 2.28	45.13 ± 1.48	48.78 ± 2.01	164.98
rac-**10**	28.98 ± 3.07	33.58 ± 2.43	41.50 ± 2.88	–	–	–	–	ND
meso-**18**	15.81 ± 2.59	22.01 ± 1.63	27.82 ± 2.81	31.16 ± 1.23	34.42 ± 0.93	–	–	ND
meso-**19**	10.22 ± 1.25	15.58 ± 0.82	22.63 ± 0.97	29.54 ± 2.3	31.24 ± 1.88	33.16 ± 0.63	40.12 ± 0.78	ND
Acarbose[c]	17 ± 0.57	25 ± 2.83	29 ± 1.01	39 ± 1.90	52 ± 0.92	60 ± 0.56	66 ± 0.72	57.78

Abbreviation: ND, not determined.

[a]Concentration required for 50% inhibition of the enzyme activity under the assay conditions.

[b]Four experiments were performed for all compounds in each experiment triplicated.

[c]Positive control.

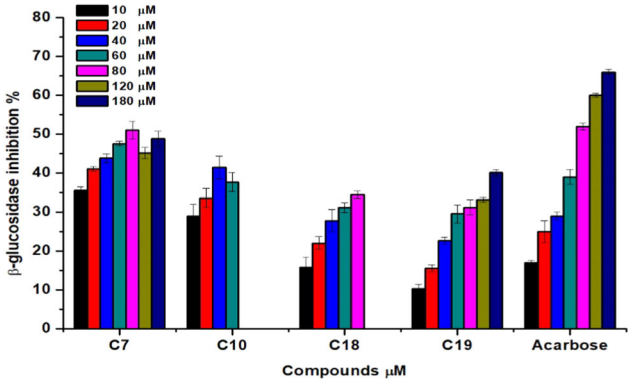

FIGURE 5 β-Glucosidase inhibition % for (10–180 µM) test compounds and acarbose control. Control of β-glucosidase inhibition % compared to acarbose concentration of C7 (**7**), C10 (**10**), C18 (**18**), and C19 (**19**) compounds. Mean values ± standard deviation are shown for triplicate experiments

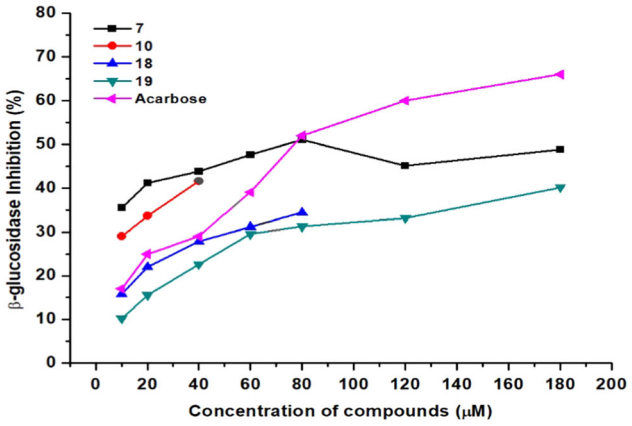

FIGURE 6 β-Glucosidase % inhibition of *rac*- and *meso*-**7**, **10**, **18**, **19**, and acarbose by different concentrations. The compounds were tested with concentrations ranging from 10 to 180 µM. Results are the means ± standard deviation of three replicates of each group

2.4 | Antimicrobial activity

The dramatic increase in multidrug-resistant microbial infections has become a serious health problem. Therefore, the search for new antimicrobial agents will remain an important and challenging task for medical chemistry.[22] The antibacterial screening indicated that all of the compounds showed varying degrees of activity against especially *P. putida* (20–23 mm; Tables 4 and 5 and Figures 7 and 8). Besides the fluorescent group of *Pseudomonas* species, *Pseudomonas putida* from other nonfermented Gram-negative organisms, which are frequently found in the environment, previously had low pathogenicity. However, in recent years, these have been seen as increasingly important human pathogens. *P. putida* causes nosocomial infections, especially in immunocompromised patients and in patients with medical devices or catheters, because they can colonize moist and lifeless hospital surfaces.[23–25] Thus, the antifungal and antimicrobial activity of the new *rac*- and *meso*-compounds (**7**, **8**, **10**, **17**, **18**, and **19**) was studied and the results are shown in Tables 4 and 5.

Some compounds and antibiotics exhibited varying degrees of inhibitory effects on the growth of the different Gram-negative and -positive pathogenic bacteria and yeast tested. The synthesized *rac*- and *meso*-compounds (**7**, **8**, **10**, **17**, **18**, and **19**) were screened for their in vitro antibacterial and antifungal activity in dimethyl sulfoxide (DMSO) at the same concentrations (0.1 µg/µl) as a test material (Tables 4 and 5).[19] The results are plotted in Figures 7 and 8 at the same concentration and in the same solvent.

The inhibition zone values of *rac*- and *meso*-compounds (**7**, **8**, **10**, **17**, **18**, and **19**) under the same conditions and in the same medium for Gram-positive and -negative bacteria are demonstrated in Figure 9.

The results of the antibacterial screening indicated that *meso*-compound **18** showed the most activity against *S. aureus* (24 mm), *P. putida*, and *P. vulgaris* (21 mm). *rac*- and *meso*-compounds **17** and **7** showed moderate activity against *S. aureus*. *S. aureus*, an adaptable pathogen, is multifaceted in nature and varies in severity of infection, affecting the skin, soft tissue, respiratory system, bone joints, and

TABLE 4 Antibacterial activities of the *rac*- and *meso*-compounds (**7**, **8**, **10**, **17**, **18**, **19**, and acarbose) in Gram-positive bacteria

	Gram-positive bacteria							
	Micrococcus luteus		*Staphylococcus epidermis*		*Staphylococcus aureus*		*Bacillus cereus*	
Compounds (µg/ml)	**100**	**200**	**100**	**200**	**100**	**200**	**100**	**200**
meso-**7**	17	17	16	20	–	12	20	14
meso-**8**	15	16	21	19	21	20	17	15
rac-**10**	15	17	17	19	–	25	12	20
rac-**17**	19	17	20	19	23	22	17	17
meso-**18**	15	20	12	20	24	21	16	18
meso-**19**	16	18	18	20	25	15	17	15
Acarbose	16	15	24	21	24	12	20	17
AMP10	22		26		30		23	
AMC30	25		27		30		20	

Abbreviations: AMC30, amoxycillin 30 µg; AMP10, ampicillin 10 µg.

TABLE 5 Antimicrobial activities of the *rac*- and *meso*-compounds (**7**, **8**, **10**, **17**, **18**, **19**, and acarbose) in Gram-negative bacteria and yeast

	Gram-negative bacteria											
	Pseudomonas putida		*Klebsiella pneumoniae*		*Enterobacter aerogenes*		*Salmonella typhi* H		*Escherichia coli*		*Proteus vulgaris*		*Candida albicans* (yeast)	
Compounds (μg/ml)	100	200	100	200	100	200	100	200	100	200	100	200	100	200
meso-**7**	18	20	13	14	14	19	20	21	18	17	20	22	11	23
meso-**8**	15	23	12	13	16	17	17	19	16	18	20	18	23	25
rac-**10**	14	23	16	15	17	18	13	22	18	18	–	14	12	22
rac-**17**	16	20	16	15	–	19	16	17	18	22	14	20	21	30
meso-**18**	13	21	15	18	19	18	16	17	20	21	21	20	20	22
meso-**19**	17	22	19	17	14	16	14	16	15	17	23	22	19	15
Acarbose	24	23	12	16	17	13	22	18	16	13	–	–	28	33
SXT25	18		20		19		17		18		19		N	
K30	14		23		24		20		25		21		N	
NYS100	N		N		N		N		N		N		20	

Abbreviations: K30, kanamycin 30 μg; N, not determined; NYS100, nystatin 100 μg; SXT25, sulfamethoxazole 25 μg.

endovascular tissues.[26,27] After the breakage of the epithelium, this extracellular pathogen bacteremia may cause serious diseases, such as pneumonia, osteomyelitis, endocarditis, and septic shock.[28] The *meso*-compound **19** showed the most activity against *S. aureus* (25 mm), *P. putida* (22 mm), and *P. vulgaris* (23 mm). *P. vulgaris* is easily isolated from patients in long-term care facilities and hospitals, and from patients with underlying diseases or with poor immune systems. The patients with repeated infection, those with constructional abnormalities in the urinary tract, those with urethral instrumentation, and those who acquired infections in the hospital have an increased density of infection caused by *Proteus* and other organisms. The *rac*-compound **17** showed the most activity against *E. coli* (22 mm) and *P. putida* (20 mm). The *meso*-compound **7** showed the most activity against *P. vulgaris* (22 mm), *S. typhi* H (21 mm), and *P. putida* (20 mm). *Salmonella* serovars cause very diverse clinical symptoms, from asymptomatic infection to serious typhoid-like syndromes, in infants or certain highly susceptible animals.[19,29,30] The *meso*-compound **8** showed the most activity against *P. putida* (23 mm), *S. epidermis* (22 mm), and *S. aureus* (22 mm). *S. epidermis* infections are associated with intravascular devices (prosthetic heart valves, etc.) but also generally occur in patients with prosthetic joints, catheters, and large wounds. These pathogenic microorganisms are continuing to gain resistance to traditional antibiotics. There is a need for more effective antibiotics for the treatment of this disease.[19,31] The *rac*-compound **10** showed the most activity against *S. aureus* (25 mm), *P. putida* (23 mm), and *S. typhi* H (22 mm) (Table 4 and Figure 8). The *rac*- and *meso*-compounds **8**, **7**, **10**, **17**, **18**, and **19** showed moderate activity against *M. luteus*, *K. pneumoniae*, *E. aerogenes*, *B. cereus*, and *E. coli*. Similarly *rac*- and *meso*-compounds **7**, **10**, **17**, **18**, and **19** showed moderate activity against *S. epidermidis*. Furthermore, the compounds **8**, **17**, **18**, and **19** showed moderate activity against *S. typhi* H. In addition, compounds *meso*-**7** and *rac*-**10** showed moderate activity against *P. vulgaris*. It was observed that the synthesized compounds were more effective against Gram(−) bacteria than against Gram(+) bacteria (Tables 4 and 5 and Figures 7–9). The *meso*-**7** and *rac*-**17** compounds showed higher activity against *M. luteus* (17 and 19 mm, respectively) than acarbose (Table 4). The *rac*-**10**, **17**, and *meso*-**7**, **17**, **18**, and **19** compounds showed higher activity against *K. pneumonia* (13, 16, 16, 15, and 19 mm, respectively) than acarbose. Further the *rac*- and *meso*-compounds (**7**, **8**, **10**, **17**, and **18**) except for one *meso*-compound (**19**) showed higher activity or same against *E. coli* (18, 16, 18, 18, and 20 mm) than acarbose (Table 5). As a result, the compounds showed greater activity in Gram-negative bacteria than acarbose (Table 5).

Systemic fungal infections, including those by *C. albicans*, have emerged as important causes of morbidity and mortality in immune-compromised patients (AIDS, cancer chemotherapy, organ or bond transplantation).[19,29] All the synthesized compounds (except for *meso*-compound **19**) demonstrated high activity against this yeast. Further, the *rac*-**17** and *meso*-**8** compounds showed the most inhibition activity against *C. albicans* as compounds with zone values of 30–23 mm. Meanwhile, the *rac*-**17** (30 mm) showed the highest activity. In fact, all the synthesized compounds (except for *meso*-**19**

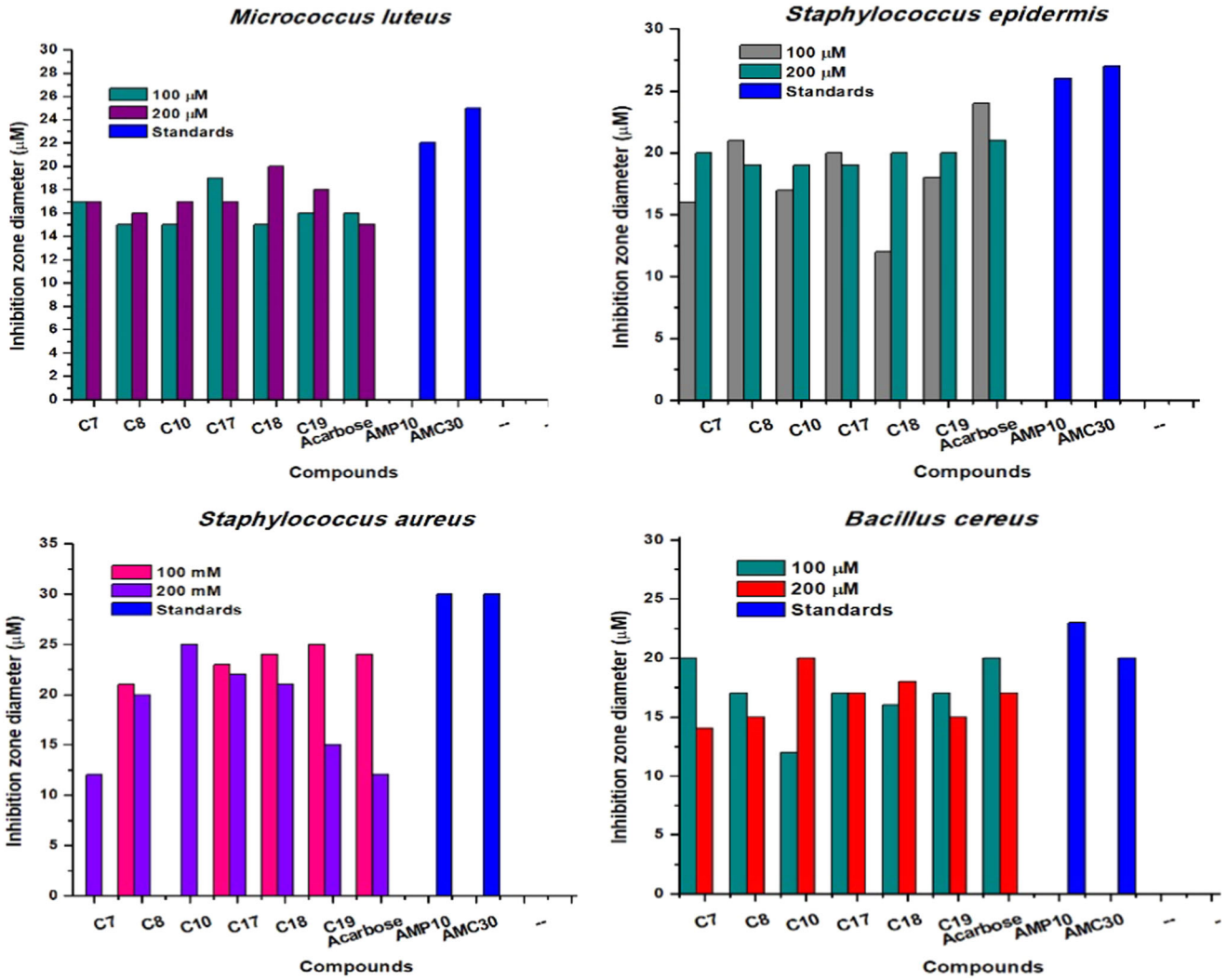

FIGURE 7 Antimicrobial activity of *rac*- and *meso*-compounds in Gram(+) bacteria (**7**, **8**, **10**, **17**, **18**, and **19**) and standard reagents (diameter of zone inhibition [mm]). AMC30, amoxycillin (30 μg); AMP10, ampicillin (10 μg); K30, kanamycin (30 μg); NYS100, nystatin (100 μg); SXT25, sulfamethoxazole (25 μg)

compound) showed more activity against *C. albicans* than the commercial (standard) antifungal (positive control NYS100; Table 5 and Figure 8).

2.5 | *S. cerevisiae* α-glucosidase molecular modeling studies

Racemic compounds **18** and **19** showed inhibition of *S. cerevisiae* α-glucosidase in the micromolar range (compound **18**: IC_{50} = 91.67 μM; compound **19**: IC_{50} = 527.39 μM), whereas the structural analogue *rac*-compound **17** and the other compounds did not show any significant inhibition (Table 2). The related *rac*- and *meso*-compounds **17**–**19** have four hydroxyl groups, whereas *meso*-compounds **7**, **8**, and *rac*-compound **10** only contain two hydroxyl groups. As such, compounds **17**–**19** have the potential to form many more hydrogen bonds with the active site of *S. cerevisiae* α-glucosidase. The *meso*- and *rac*-molecules **7**, **8**, **10**, **17**, **18**, and **19**, as well as maltose, obtained from the crystal structure active site, were docked into the active site of *S. cerevisiae* α-glucosidase. The docked pose of the endogenous substrate maltose was very similar to its binding pose as observed in the crystal structure (root mean standard deviation: 0.6830 Å). Both poses form hydrogen-bonding interactions with the side chains of Asp69, His112, Arg213, Glu277, His351, Asp352, and Arg442 (Figure 10). The only difference is in the orientation of the maltose O6 oxygen atom, which in the crystal structure forms a hydrogen bond with Asp215 via its hydrogen atom, whereas in the docked pose this hydrogen bond is formed with Asp69. Interestingly, the docked pose of maltose has the best-calculated score (−29.4360) among all the docked ligands.

The docked pose of *meso*-compound **18** shows that the six-membered ring of the compound is located between Asp69 and Glu277 and forms two hydrogen bonds with each of the amino acids (Figure 11). The docked pose of *meso*-compound **19** indicates that the cyclohexyl group of this compound adopts similar to the six-ring of maltose (Figure 12). In addition, hydrogen bonds are

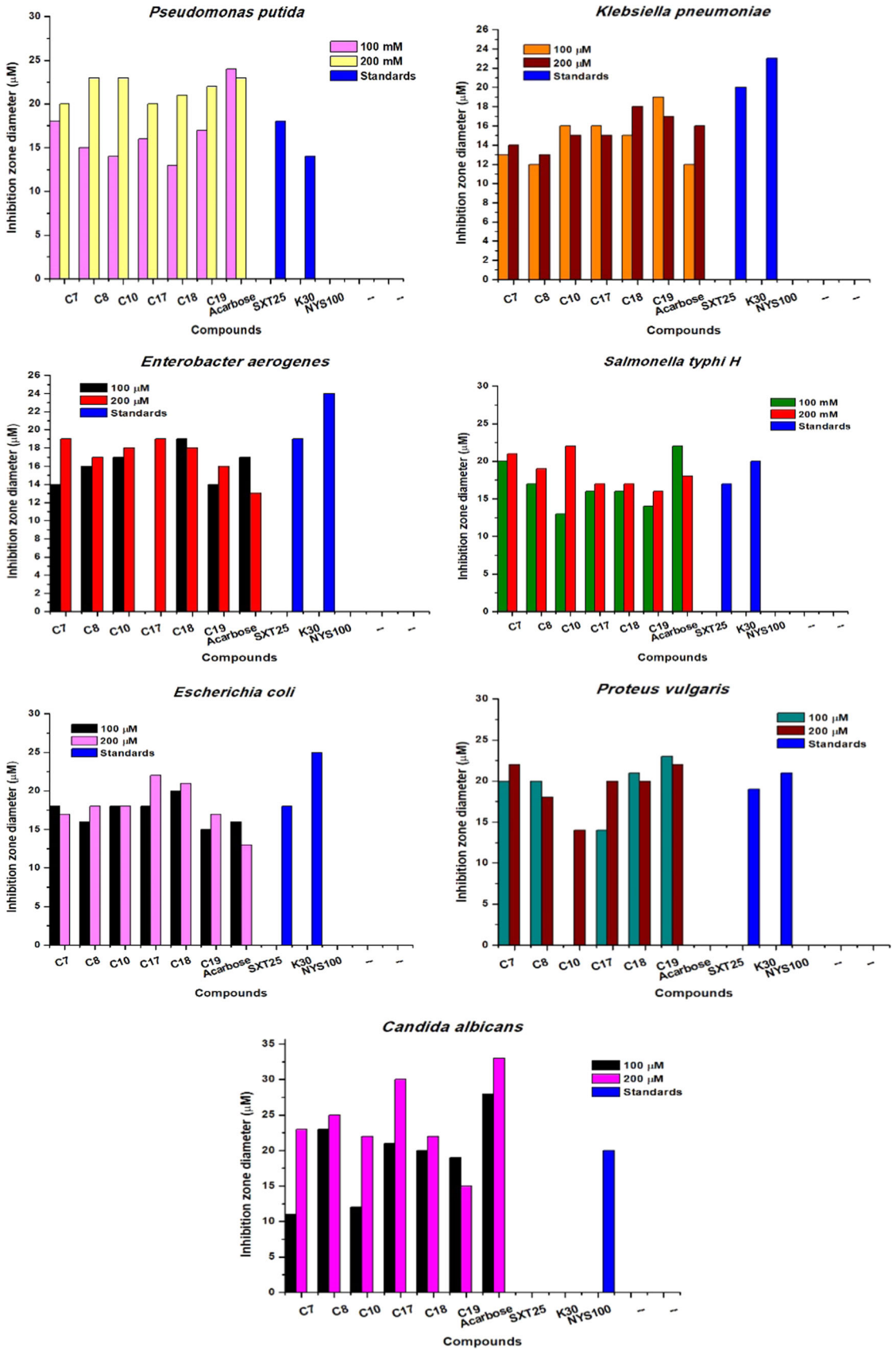

FIGURE 8 Antimicrobial activity of *rac*- and *meso*-compounds in Gram(−) bacteria, yeast (**7**, **8**, **10**, **17**, **18**, and **19**)) and standard reagents (diameter of zone inhibition [mm]). AMC30, amoxycillin (30 µg); AMP10, ampicillin (10 µg); K30, kanamycin (30 µg); NYS100, nystatin (100 µg); SXT25, sulfamethoxazole (25 µg)

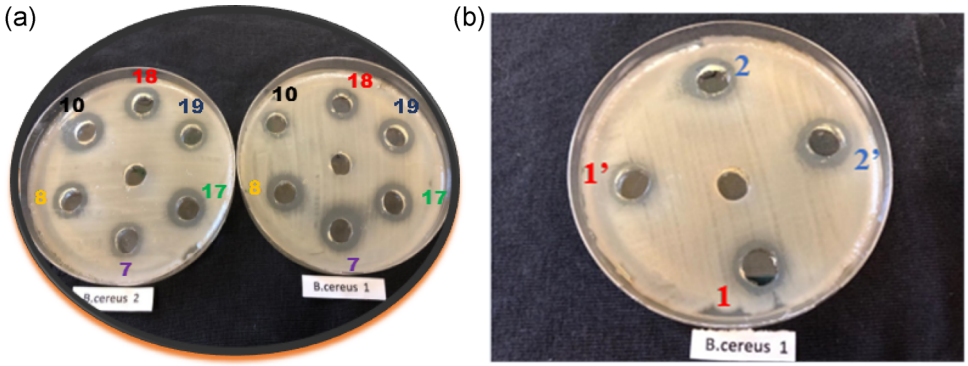

FIGURE 9 Antimicrobial activity (inhibition zone [mm]) of *rac*- and *meso*-compounds in Gram(−) and Gram(+) bacteria and yeast (**7**, **8**, **10**, **17**, **18**, **19**, and acarbose). (a) *Bacillus cereus* 1 = 100 μM and *B. cereus* 2 = 200 μM. (b) 1 = 100 μM, 1′ = duplicated for 100 μM, 2 = 200 μM and 2′ = duplicated for 200 μM for acarbose

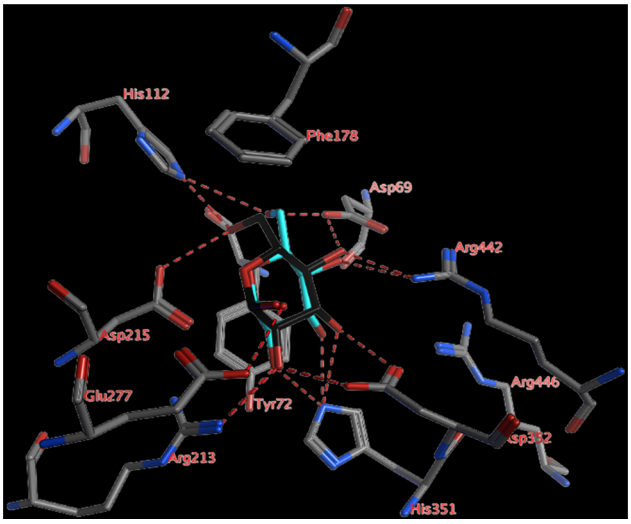

FIGURE 10 Comparison of the docked pose (turquoise) and the binding pose (black) of maltose as observed in the active site of *Saccharomyces cerevisiae* α-glucosidase. Hydrogen bonds are indicated with red dashed lines

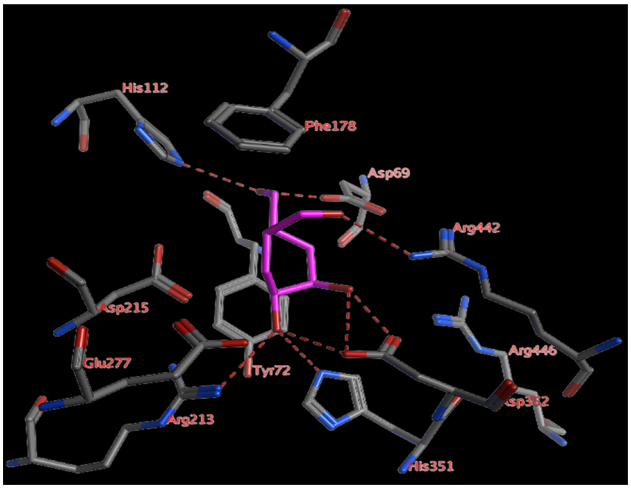

FIGURE 12 The docked pose of *meso*-compound **19** (purple) in the active site of *Saccharomyces cerevisiae* α-glucosidase. Hydrogen bonds are indicated with red dashed lines

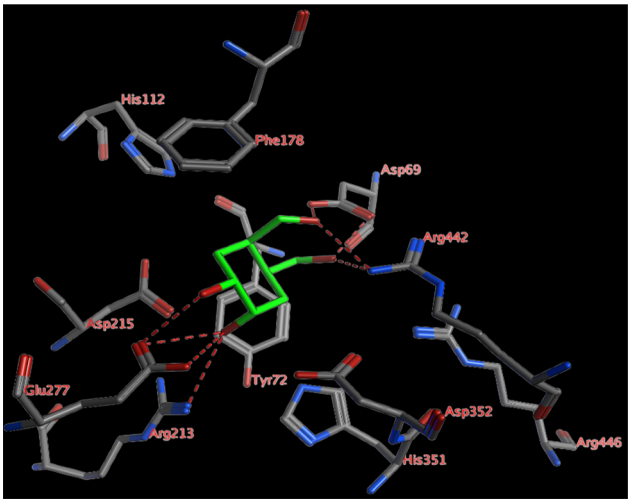

FIGURE 11 The docked pose of *meso*-compound **18** (green) in the active site of *Saccharomyces cerevisiae* α-glucosidase. Hydrogen bonds are indicated with red dashed lines

formed between *meso*-compound **19** and the side chains of Asp69, His112, Arg213, His351, Asp352, and Arg442. Compared to the reference ligand maltose, the only hydrogen bond that is not formed is with Glu277.

The docked poses of *meso*-compounds **7**, **8**, and *rac*-compound **10** indicate that these compounds can form fewer interactions with the active site compared to *meso*-compounds **18** and **19**. As such, their binding affinity to the active site is expected to be less compared to *meso*-compounds **18** and **19**. The *rac*-compound **17** is not able to form similar interactions as observed for its structural analogues *meso*-**18** and *meso*-**19** and the interactions with the enzyme are less optimal and it forms fewer hydrogen bonds (Figure 13).

The observed differences in the poses of *meso*-compounds **7**, **8**, and *rac*-compounds **10**, **17** compared to the docked poses of *meso*-compounds **18** and **19** may explain the lower affinity, and thus, the activity of the former compounds (Table 2).

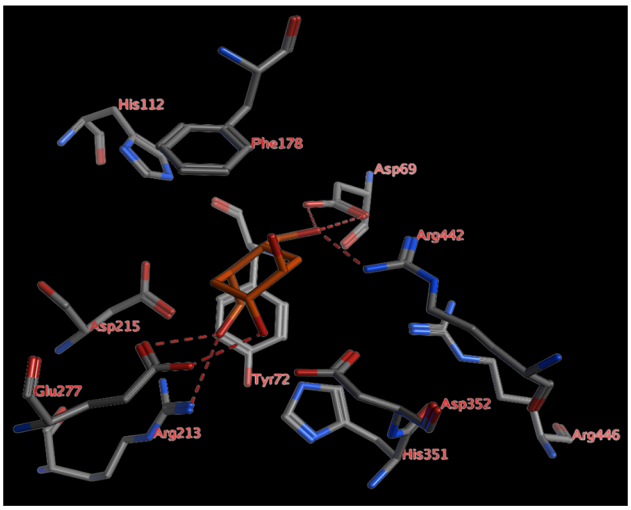

FIGURE 13 The docked pose of *rac*-compound **17** (brown) in the active site of *Saccharomyces cerevisiae* α-glucosidase. Hydrogen bonds are indicated with red dashed lines

2.6 | Similarity between the active sites of α-glucosidases

The overall sequences of α-glucosidases from *Homo sapiens* (Q07837.2), *Mycobacterium tuberculosis* H37Rv (P9WQ18.1), *Neisseria meningitidis* (Q84HD6.1), *C. albicans* (Q02751.4), *E. coli* K12 (P21517.5), *Streptococcus pneumoniae* TIGR4 (Q54796.2), and *Streptococcus mutans* UA159 (Q99040.2) were compared to the sequence of *S. cerevisiae* α-glucosidase. The highest sequence identity was found for *C. albicans* (48%) and the two *Streptococcus* enzymes (32%). The lowest identity was found for *E. coli* (10%) and *N. meningitidis* (13%), whereas the human and *M. tuberculosis* enzymes showed 23% and 20% identity, respectively.

The sequence identity of the active site residues, which were defined as all residues in the *S. cerevisiae* α-glucosidase active site that either form hydrogen bonds or direct hydrophobic contacts to either maltose or the docked compounds (Asp69, Tyr72, His112, Phe178, Arg213, Asp215, Glu277, His351, Asp352, and Arg442) was much higher. The active sites of *C. albicans* and the two *Streptococcus* enzymes showed 100% identity, the human and *N. meningitidis* active sites showed 70% identity, the *M. tuberculosis* active site showed 60% identity, and the *E. coli* active site showed 30% identity with the *S. cerevisiae* α-glucosidase active site. The identity data indicate that these compounds may also bind to α-glucosidase enzymes from humans and several pathogenic organisms such as *S. pneumoniae*, *S. mutans*, *N. meningitidis*, and *M. tuberculosis*.

3 | CONCLUSION

The aim of this study was to add to the literature on different tetrol isomers. The double bond of the initial hexahydroisobenzofuran **6** was oxidized by *m*-CPBA and OsO_4 for *trans*- and *cis*-hydroxylation and then hydrolyzing of the hydrofuran ring for forming carbohydrate structures containing the tetra hydroxyl group in the cyclohexane skeleton. In the study, on epoxidation of the double bond of the starting compound **6** with *m*-CPBA, theoretically two different epoxide products were expected to form, but only the single *meso*-epoxide isomer **9** was formed stereospecifically. Conversion of the epoxide with H^+/H_2O gave the *rac*-diol-hydrofuran **10**, which was converted to diacetate **11** by esterification. Then the furan ring was exposed to ring cleavage with the Ac_2O/AcOH couple in the presence of a catalyst (H_2NSO_3),[13b,c] which afforded scaffold **14**. By the same way, after oxidation of the double bond of the starting compound **6** with OsO_4, two *cis*-diol-hydrofuran *meso*-isomers **7** and **8**, were afforded. Considering the difficulties in isolating and purifying the resulting *meso-cis*-diol furans **7** and **8**, the diol groups were protected by esterification and then isolated to afford diacetate furan stereoisomers **11** and **12**. The furan ring was opened with the Ac_2O/AcOH couple in the presence of a catalyst (H_2NSO_3) to afford stereoisomers **15** and **16**. Deacetylation of tetraacetates **14–16** with NH_3 (g) gave *rac*- and *meso*-tetrols **17–19**. Thus, the new tetrol isomers formed were introduced into the literature.

The synthesized all *rac*- and *meso*-compounds (**7**, **8**, **10**, **17**, **18**, and **19**) exhibited antibacterial and antifungal activities at moderate to good levels against both Gram-negative and -positive bacteria (Tables 4 and 5 and Figures 7 and 8). The antimicrobial activity of the compounds was also compared with commercial (standard) antibiotics. It was seen that the synthesized compounds were as effective as the antibiotics and antifungal mentioned. Furthermore, some of the synthesized compounds (*P. putida*; all compounds, 20–23 mm) were more effective than the antibiotics and antifungal (*C. albicans*; all compounds [except for *meso*-compound **19**][19]; 21–30 mm; Figure 9).

In the molecular docking study, the three-dimensional structures of *rac*- and *meso*-compounds **7**, **8**, **10**, **17**, **18**, and **19** were constructed using the MOE software package, with energy minimized using a steepest-descent protocol. The identity data indicate that these compounds may also bind to α-glucosidase enzymes from humans and several pathogenic organisms such as *S. pneumoniae*, *S. mutans*, *N. meningitidis*, and *M. tuberculosis*.

4 | EXPERIMENTAL

4.1 | Chemistry

4.1.1 | General

In the experiment, for solvent removal Heidolph Laborota 4001 and Bibby rotary evaporator were used. Heidolph MR Hei-standard heating stirrers were used as the heat source. Chemicals and solvents were purchased from commercial suppliers. The spectra (NMR, COSY, and HETCOR) were recorded at 300 MHz for ^{1}H-NMR and 75 MHz for ^{13}C-NMR spectrometer (see the Supporting Information for the original spectra). Proton chemical shifts are reported in ppm (δ) using TMS (δ, 0.0 ppm) as reference. Chemical shifts were given as multiplicity (singlet [s], doublet [d], triplet [t], quartet [q], multiplet [m], broad [br]) and coupling constants were given in Hz. Infrared spectra were recorded with a Perkin-Elmer 1600 FT-IR (4,000–400 cm^{-1}) spectrometer. Melting points (MPs) were

performed in capillary. Column chromatography was realized on silica gel (60-mesh, Merck). For proceeding reaction controls, thin-layer chromatography (TLC on Merck 0.2 mm silica gel 60 F254 analytical aluminum plates) was used.

The InChI codes of the investigated compounds together with some biological activity data are provided as Supporting Information.

4.1.2 | Synthesis of hydroxylation products with OsO_4

Hexahydroisobenzofuran **6** (3.7 g, 29.80 mmol) was dissolved in of acetone (20 ml) and water (20 ml). *N*-Methyl Imorpholine-*N*-oxide (5.24 g, 44.69 mmol) was added to the stirred solution. OsO_4 solution (10 ml of 60%) prepared in aceton was injected at 0°C in N_2 atmosphere. The mixture was stirred magnetically for 48 hr at room temperature. The reaction was controlled with ^{1}H-NMR spectra. After completion of the reaction pH was adjusted to 2 approximately with HCl, and the mixture was worked up with EtOAc, dried on Na_2SO_4. The organic solution was evaporated, the residue was separated on column with silica gel with EtOAc/hexane, 1:4 ratio, the separation procedure was repeated and the same fraction was collected afforded two stereoisomer **7** and *meso*-**8**, respectively.

*The first stereoisomer meso-**7***

Yield (3 g, 63.7%) as a white solid. MP: 98°C. ^{1}H-NMR (300 MHz, $CDCl_3$): δ (ppm) = 3.85 (m, 3H, H_1 or H_2 and $H_{5a5a'}$ or $H_{4a4a'}$), 3.60 (dd, $J_{5a5a'}$ or $_{4a4a'}$ = 8.2 Hz, $J_{5a5a'}$ or $_{4a4a'}$ = 5.6 Hz, 2H, H_{5a} and $H_{5a'}$ or H_{4a} and $H_{4a'}$), 2.46 (ddd, J = 16.6 Hz, 12.3 Hz, 6.1 Hz, 2H, H_5 and H_4), 2.10 (bs, 2H, 2(–OH)), 1.95 (ddd, J = 13.8, 7.3, 6.5 Hz, 2H, $H_{6'6}$ and $H_{3'3}$), and 1.63 (dq, J = 14.0, 3.8 Hz, 2H, $H_{6'6}$ and $H_{3'3}$). ^{13}C-NMR (75 MHz, $CDCl_3$): δ (ppm) = 71.8, 68.7, 35.6, and 28.9. Infrared (IR; KBr): 3,346, 2,940, 2,889, 1,269, 1,028, 885, 639, and 539. Anal. calcd. for $C_8H_{14}O_3$: C, 60.74; H, 8.92; O, 30.34. Found: C, 60.82, H, 8.61; O, 30.32.

*The second stereoisomer meso-**8***

Yield (1.4 g, 29.7%) as a colorless viscous. ^{1}H-NMR (300 MHz, $CDCl_3$/CD_3OD: 5:1): δ (ppm) = 3.76 (m, 6H, H_1, H_2 and $H_{5a5a'}$, $H_{4a4a'}$), 3.28 (m, 2H, –OH), 2.17 (m, 2H, H_4 and H_5), and 1.81 (m, 2H, H_6 or H_3). ^{13}C-NMR (75 MHz, $CDCl_3$/CD_3OD: 5:1): δ (ppm) = 72.6, 69,6, 37.1, and 28.4. IR (KBr): 3,369, 2,917, 2,879, 1,311, 1,039, 878, 648, and 414. Anal. calcd. for $C_8H_{14}O_3$: C, 60.74; H, 8.92; O, 30.34. Found: C, 60.55, H, 8.72; O, 30.45.

4.1.3 | Synthesis of (3a*R*,5*S*,6*R*,7a*S*)-octahydroisobenzofuran-5,6-diyl diacetate 12 and (3a*R*,5*R*,6*S*,7a*S*)-octahydroisobenzofuran-5,6-diyl diacetate 13

Compound **7** (3 g, 18.96 mmol) was dissolved in pyridine (3 ml) and was added Ac_2O (5 ml). The mixture was stirred at room temperature for 24 hr. The excess pyridine and Ac_2O was hydrolyzed with HCl (5%) in ice water. DCM (100 ml) was added and the mixture was extracted with, water, saturated aqueous $NaHCO_3$ solution, dried on Na_2SO_4, respectively. The solution was removed in vacuum under reduced pressure (20°C, 25mmHg) to give (3a*R*,5*S*,6*R*,7a*S*)-octahydroisobenzofuran-5,6-diyl diacetate **12** as a colorless liquid. To obtain compound *meso*-**8** (1.40 g, 8.85 mmol) the same procedure for the synthesis of **7** was used to give (3a*R*,5*R*,6*S*,7a*S*)-octahydroisobenzofuran-diethyl diacetate **13** as a white solid.

*(3a*R*,5*S*,6*R*,7a*S*)-Octahydroisobenzofuran-5,6-diyl diacetate **12***

Yield (4.3 g, 93.6%) as a colorless liquid. ^{1}H-NMR (300 MHz, $CDCl_3$): δ (ppm) = 5.12 (dd, J = 6.5 Hz, 2.9 Hz, 1H, H_1 and H_2), 3.87 (dd, J = 8.5 Hz, 5.3 Hz, 2H, H_{5a}, H_{4a} or $H_{5a'}$, $H_{4a'}$), 3.66 (dd, J = 8.2 Hz, 6.8 Hz, 2H, $H_{5a'}$, $H_{4a'}$ or H_{5a}, H_{4a}), 2.49 (ddd, J = 14.5, 10.5, 6.2 Hz, 2H, H_5 and H_4), 2.07 (s, 9H), 2.04 (dtd, J = 14.4, 5.9, 2.0 Hz, 2H, H_{6a}, H_{3a}, or $H_{6a'}$, $H_{3a'}$), and 1.73 (dq, J = 14.5, 4.1 Hz, 2H, $H_{6a'}$, $H_{3a'}$, or H_{6a}, H_{3a}). ^{13}C-NMR (75 MHz, $CDCl_3$): δ (ppm) = 170.6, 71.5, 69.0, 35.8, 26.7, and 21.4. IR (KBr): 2,938, 2,870, 1,736, 1,441, 1,367, 1,227, 1,026, and 895. Anal. calcd. for $C_{12}H_{18}O_5$: C, 59.49; H, 7.49; O, 33.02. Found: C, 59.65; H, 7.26, O, 33.22.

*(3a*R*,5*R*,6*S*,7a*S*)-Octahydroisobenzofuran-5,6-diyl diacetate **13***

Yield (1.53 g, 71.36%) as a white solid. MP: 61°C. ^{1}H-NMR (300 MHz, $CDCl_3$): δ (ppm) = 5.09–5.05 (m, 2H, H_1 and H_2), 3.89–3.78 (m, 4H, H_{5a} and H_{4a}), 2.36 (m, 2H, H_4 and H_5), 2.04 (s, 6H), 2.03–1.93 (m, 2H, H_6 or H_3), and 1.86–1.82 (m, 2H, H_3 or H_6). ^{13}C-NMR (75 MHz, $CDCl_3$): δ (ppm) = 170.6 (2C), 72.4 (2C), 70.0 (2C), 37.0 (2C), 26.7 (2C), and 21.4 (2C). IR (KBr): 2,928, 2,879, 1,734, 1,434, 1,368, 1,242, 1,043, and 898. Anal. calcd. for $C_{12}H_{18}O_5$: C, 59.49; H, 7.49; O, 33.02. Found: C, 59.43; H, 7.48, O, 33.17.

4.1.4 | Synthesis of (1*R*,2*S*,4*R*,5*S*)-4,5-bis-(acetoxymethyl)cyclohexane-1,2-diyl diacetate 16

To the (3a*R*,5*S*,6*R*,7a*S*)-oktahydroisobenzofuran-5,6-diyl diacetate **13** (1.40 g, 5.78 mmol), Ac_2O/AcOH (15 ml; 1:1) was added at room temperature, then catalytic amount of H_2NSO_3H (112 mg, 1.16 mmol). The mixture was stirred at reflux temperature for 24 hr. The mixture was brought to room temperature and controlled with TLC. After completion of the reaction, it was hydrolyzed by addition of water (200 ml) and ether (200 ml), respectively. The ether phase was washed three times with water (100 ml) and saturated $NaHCO_3$ (100 ml), dried on anhydrous $MgSO_4$. The organic phase was removed by evaporation and the residue was purified with silica gel column using silica (20 g) with EtOAc/hexane (1:2), which gave (1*R*,2*S*,4*R*,5*S*)-4,5-bis(acetoxymethyl)cyclohexane-1,2-diyl diacetate **16** (1.55 g, 78%) as sole product, colorless and viscous. ^{1}H-NMR (300 MHz, $CDCl_3$): δ (ppm) = 5.05 (m, 2H, H_1 and H_2), 4.18–4.04 (m, 4H, H_{4a} and H_{5a}), 2.21–2.09 (m, 2H, H_4 and H_5), 2.04 (s, 6H), 2.03 (s, 6H), 1.93 (m, 2H, H_6 or H_3), and 1.71 (dm, J = 10.2, 3.8 Hz, 2H, H_3 or H_6). ^{13}C-NMR (75 MHz, $CDCl_3$): δ (ppm) = 171.1 (2C), 170.4 (2C),

70.3 (2C), 65.1 (2C), 24.0 (2C), 27.5 (2C), 21.3 (2C), and 21.1 (2C). IR (KBr): 2,953, 1,732, 1,368, 1,224, 1,033, and 605. Anal. calcd. for $C_{16}H_{24}O_8$: C, 55.81; H, 7.03; O, 37.17. Found: C, 55.57; H, 7.23, O, 37.35.

4.1.5 | Synthesis of (1*R*,2*S*,4*R*,5*S*)-4,5-bis-(hydroxymethyl)cyclohexane-1,2-diol 19

1,2-Diyl diacetate **16** (0.4 g, 1.16 mmol), was dissolved in absolute methanol (15 ml). Dry NH_3 (g) was passed through the resulting solution for 1 hr at room temperature and the reaction flask was closed with stopper. The mixture was stirred at room temperature for 12 hr controlling with TLC. After the reaction was complete, the solvent and the forming acetamide were removed in vacuum to give *meso*-tetrol **19** (0.18 g, 88%) as brown and viscous. ^{1}H-NMR (300 MHz, $CD_3OD/CDCl_3$: 5:1): δ (ppm) = 4.50 (bs, 4H, 4×(–OH)), 3.62 (m, 6H, H_1, H_2 and $H_{5a5a'}$, $H_{4a4a'}$), 1.85 (m, 2H, H_4 and H_5), 1.74 (m, 2H, H_3 or H_6), and 1.64 (m, 2H, H_6 or H_3). ^{13}C-NMR (75 MHz, $CD_3OD/CDCl_3$: 5:1): δ (ppm) = 69.9, 63.3, 37.3, and 30.3. IR (KBr): 3,293, 2,879, 1,663, 1,433, 1,213, 1,018, and 546. Anal. calcd. for $C_8H_{16}O_4$: C, 54.53; H, 9.15; O, 36.32. Found: C, 54.15; H, 8.77, O, 36.70.

4.1.6 | Synthesis of (1*R*,2*S*,4*S*,5*R*)-4,5-bis-(acetoxymethyl)cyclohexane-1,2-diyl diacetate 15

To the (3a*R*,5*R*,6*S*,7a*S*)-oktahydroizobenzofuran-5,6-diyl diacetate **12** (0,9 g, 3.71 mmol), Ac_2O/AcOH (15 ml: 1:1) was added at room temperature. The catalytic amount of H_2NSO_3H (72 mg, 0.74 mmol) was added. The procedure above for **16** was used to give (1*R*,2*S*,4*S*,5*R*)-4,5-bis(acetoxymethyl)cyclohexane-1,2-diyl diacetate **15** (1.02 g, 80%) as a colorless liquid. ^{1}H-NMR (300 MHz, $CDCl_3$): δ (ppm) = 5.12 (bs, 2H, H_1 and H_2), 4.04 (t, 4H, J = 4.9 Hz, H_{5a} and H_{4a}), 2.35–2.05 (m, 2H, H_5 and H_4), 2.03 (bs, 3H), 2.02 (bs, 9H), 1.81–1.89 (m, 2H, H_6, $H_{6'}$ or H_3, $H_{3'}$), and 1.72–1.80 (m, 2H, H_3, $H_{3'}$ or H_6, $H_{6'}$). ^{13}C-NMR (75 MHz, $CDCl_3$): δ (ppm) = 171.1, 170.5, 68.5, 64.4, 33.1, 28.2, 21.3, and 21.1. IR (KBr): 2,937, 1,713, 1,370, 1,235, 1,033, and 607. Anal. calcd. for $C_{16}H_{24}O_8$: C, 55.81; H, 7.03; O, 37.17. Found: C, 55.62; H, 7.11, O, 37.42.

4.1.7 | Synthesis of (1*R*,2*S*,4*S*,5*R*)-4,5-bis-(hydroxymethyl)cyclohexane-1,2-diol 18

Tetraacetate **15** (0.3 g, 1.16 mmol) was dissolved absolute methanol as above for the synthesis of **19**, to give (1*R*,2*S*,4*S*,5*R*)-4,5-bis-(hydroxymethyl)cyclohexane-1,2-diol as a brown liquid *meso*-**18** (0.14 g, 92%). ^{1}H-NMR (300 MHz, D_2O): δ (ppm) = 4.65 (s, 4H, 4×(OH)), 3.72 (m, 2H, H_1 and H_2), 3.42 (dd, A part of AB system $J_{5a5a'}$ = 11.2 Hz, J_{5a5} = 6.2 Hz, 2H, $H_{5a'}$, H_5 or H_{4a}, $H_{4a'}$, H_4), 3.32 (dd, B part of AB system $J_{5a'5a}$ = 11.2 Hz, J_{5a5} = 7.6 Hz, 2H, $H_{5a'}$, H_5 or H_{4a}, $H_{4a'}$, H_4), 1.93 (bs, 1H, H_3 or H_5 or H_6), 1.90 (m, 2H, H_3, H_5, H_6), and 1.50 (m, 3H, H_3, H_5 and H_6). ^{13}C-NMR (75 MHz, D_2O): δ (ppm) = 68.0, 62.0, 35.3, and 28.9. IR (KBr): 3,337, 2,930, 1,665, 1,373, 1,249, 1,028, and 522. Anal. calcd. for $C_8H_{16}O_4$: C, 54.53; H, 9.15; O, 36.32. Found: C, 54.67; H, 8.48, O, 36.55.

4.1.8 | Synthesis of (1a*R*,2a*R*,5a*S*,6a*S*)-octahydroxyreno[2,3-*f*]isobenzofuran 9

To a solution of hexahydroisobenzofuran **6** (2.8 g, 22.55 mmol) in DCM (75 ml) was added a solution of *m*-chloroperbenzoic acid (*m*-CPBA; 6.67 g, 27.06 mmol, 70%). The resulting mixture was stirred magnetically at room temperature for 48 hr, then $NaHSO_3$ solution (100 ml, 50%) was added, and the mixture was stirred for 15 min. The organic layer was separated, washed with water (2 × 200 ml), and saturated aqueous $NaHCO_3$ (2 × 100 ml) dried (Na_2SO_4). After removal of the solvent under reduced pressure to give the mono-epoxy isobenzofuran **9** (2.56 g, 81%) as a yellow liquid and a single product. ^{1}H-NMR (300 MHz, C_6D_6): δ (ppm) = 3.56 (dd, A part of AB system $J_{5a5a'}$ or $_{4a4a'}$ = 8.0 Hz, J_{5a5} or $_{4a4}$ = 6.8 Hz, 2H, H_{5a} or $_{5a'}$ and $_{a}$ or $_{4a'}$), 3.16 (dd, B part of AB system $J_{5a'5a}$ or $_{4a'4a}$ = 8.0 Hz, J_{5a5} or $_{4a4}$ = 5.6 Hz, 2H, $H_{5a'}$ or $_{5a}$ and $H_{4a'}$ or $_{4a}$), 2.64 (bs, 2H, H_1 and H_2), 1.88 (ddd, J = 18.4, 13.7, 6.7H, 2H, H_4 and H_5), 1.72 (dd, A part of AB system $J_{65(6'5)}$ or $_{34(3')}$ = 15.8 Hz, $J_{66'}$ or $_{33'}$ = 6.1 Hz, 2H, H_6 or $H_{6'}$ and H_3 or $H_{3'}$), 1.19 (dd, B part of AB system, $J_{34(34')}$ or $_{65(65')}$ = 15.5 Hz, and $J_{6'6}$ or $_{3'}$ = 6.1 Hz, 2H, $H_{3'}$ or H_3 and $H_{6'}$ or H_6). ^{13}C-NMR (75 MHz, C_6D_6): δ (ppm) = 73.4, 51.2, 32.7, and 23.8. IR (KBr): 3,409, 2,923, 2,853, 1,718, 1,428,1,255, 1,019, and 750. Anal. calcd. for $C_8H_{12}O_2$: C, 68.55; H, 8.63; O, 22.83. Found: C, 68.73; H, 8.52, O, 22.61.

4.1.9 | Synthesis of (3a*R*,5*R*,6*R*,7a*S*)-octahydroisobenzofuran-5,6-diol 10

Epoxide **9** (0.5 g, 3.57 mmol) was dissolved in water (15 ml) and H_2SO_4 (69.96 mg, 0.71 mmol) was added. The mixture was stirred at room temperature overnight. $NaHCO_3$ was slowly added to neutralize the acid. The solution was stirred for 15 min. After the removal of water, the residue was filtered through a short column of silica gel (5 g) with absolute methanol. *rac*-**10** was obtained (0.4 g, 70.9%) as a colorless viscous product. ^{1}H-NMR (300 MHz, $CDCl_3$): δ (ppm) = 3.96 (bs, 2H, –OH), 3.89 (t, J = 8.2 Hz, 1H), 3.86 (dd, J = 13.0 Hz, J = 4.4 Hz, 1H), 3.66 (t, J = 5.2 Hz, 1H), 3.64 (t, J = 11.0 Hz, 1H), 3.51 (dq, J = 11.0 Hz, J = 4.7 Hz, 1H), 3.37 (m, 1H), 2.51 (m, 1H, H_4), 2.28 (dt, J = 11.4 Hz, 5.6 Hz, 1H, H_5), 2.00 (dd, J = 13.8 Hz, 3.2 Hz, 1H, H_3 or $H_{3'}$), 1.91 (dt, J = 13.2 Hz, 5.0 Hz, 1H, H_6 or $H_{6'}$), 1.64 (dq, J = 13.8 Hz, 5.9 Hz, 1H, $H_{3'}$ or H_3), and 1.40 (q, J = 12.6 Hz, 1H, $H_{6'}$ or H_6). ^{13}C-NMR (75 MHz, $CDCl_3$): δ (ppm) = 74.2, 74.1, 69.5, 38.3, 38.2, 33.5, and 30.1. IR (KBr): 3,318, 2,929, 2,861, 1,240, 1,027, 880, 658, and 502. Anal. calcd. for $C_8H_{14}O_3$: C, 60.74; H, 8.92; O, 30.34. Found: C, 60.98, H, 8.54; O, 30.76.

4.1.10 | Synthesis of (3a*R*,5*R*,6*R*,7a*S*)-octahydroisobenzofuran-5,6-diyl diacetate 11

Compound **10** (0.4 g, 2.53 mmol) was dissolved in pyridine (3 ml) and Ac_2O (6 ml) was added. The reaction was carried out with the same procedure for the synthesis of **12** to give compound **11** (0.5 g, 81.6%) was obtained as a yellow liquid. ^{1}H-NMR (300 MHz, $CDCl_3$): δ (ppm) = 5.01 (ddd, J = 13.7, 11.0, 5.0 Hz, 1H, H_2), 4.87 (ddd, J = 11.0, 8.8, 4.4 Hz, 1H, H_1), 3.91 (t, J = 8.5 H, 1H, –CH_2–, H_{5a} or $H_{5a'}$), 3.84 (dd, J = 8.5, 5.3 Hz, 1H, –CH_2–, $H_{5a'}$ or H_{5a}), 3.70 (t, J = 9.1 Hz, 1H, –CH_2–, H_{4a} or $H_{4a'}$), 3.65 (dd, J = 8.8, 2.1 Hz, 1H, –CH_2–, $H_{4a'}$ or H_{4a}), 2.51 (ddd, J = 14.9, 9.7, 5.9 Hz, 1H, H_5), 2.36 (dtd, J = 7.6, 5.9, 2.1 Hz, 1H, H_4), 2.55–2.05 (m, 2H, –CH_2–, H_6 and H_3), 2.04 (bs, 6H, 2×(–CHOAc), 1.77 (ddd, J = 14.3, 10.0, 5.9 Hz, 1H, –CH_2–, H_6), and 5.59 (dt, J = 13.2, 10.9, Hz, 1H, –CH_2–, H_3). ^{13}C-NMR (75 MHz, $CDCl_3$): δ (ppm) = 170.62, 170.59, 73.5, 72.5, 70.5, 70.0, 37.4, 37.2, 30.2, 27.8, 21.4, and 21.3. IR (KBr): 2,938, 2,873, 1,731, 1,434, 1,368, 1,224, 1,037, and 975. Anal. calcd. for $C_{12}H_{18}O_5$: C, 59.49; H, 7.49; O, 33.02. Found: C, 59.82; H, 7.41, O, 33.40.

4.1.11 | Synthesis of (1*R*,2*R*,4*R*,5*S*)-4,5-bis-(acetoxymethyl)cyclohexane-1,2-diyl diacetate 14 from 9 and 11

To the mono-epoxy hydro-isobenzofuran **9** (0.65 g, 4.64 mmol), Ac_2O/AcOH (15 ml; 1:1) was added at room temperature. The catalytic amount of H_2NSO_3H (90 mg, 0.92 mmol) was added. The procedure above for **16** was used to give (1*R*,2*R*,4*R*,5*S*)-4,5-bis-(acetoxymethyl)cyclohexane-1,2-diyl diacetate **14** (1.33 g, 83%) as a colorless viscous. ^{1}H-NMR (300 MHz, $CDCl_3$): δ (ppm) = 4.98 (ddd, J = 10.2, 8.6, 4.4 Hz, 1H, H_1 or H_2), 4.88 (dt, J = 8.6, 4.7 Hz, 1H, H_2 or H_1), 4.16–3.96 (m, 4H, H_4 and H_{5a}), 2.33 (m, 2H, H_4 and H_5), 2.27–1.98 (m, 3H, H_3 and H_6), 2.08 (s, 3H), 2.06 (s, 3 H), 2.04 (s, 6H), and 1.62–1.53 (m, 1H, H_3 and H_6). ^{13}C-NMR (75 MHz, $CDCl_3$): δ (ppm) = 171.1 (2C), 170.6, 170.4, 72.7, 70.2, 65.3, 63.2, 36.0, 33.8, 30.9, 28.8, 21.3, 21.2 (2C), and 21.1. IR (KBr): 2,956, 1,732, 1,368, 1,224, 1,033, and 605. Anal. calcd. for $C_{16}H_{24}O_8$: C, 55.81; H, 7.03; O, 37.17. Found: C, 55.72; H, 7.23, O, 37.28.

Also, starting from compound **11** (0.5 g, 2.06 mmol), 15 ml of Ac_2O/AcOH (1:1) was added at room temperature. Then catalytic amount of H_2NSO_3H (40 mg, 0.41 mmol) was added and hydrolyzed as described above for the synthesis of **16** to give compound **14** (0.59 g, 83%).

4.1.12 | Synthesis of (1*R*,2*R*,4*R*,5*S*)-4,5-bis-(hydroxymethyl)cyclohexane-1,2-diol 17

Hydrolysis of compound **14** (0.45 g, 1.31 mmol) was realized as described above for the synthesis of *meso*-**19**, to afford the (1*R*,2*R*,4*R*,5*S*)-4,5-bis(hydroxymethyl)cyclohexane-1,2-diol **17** (0.12 g, 91%) as a dark yellow and viscous. ^{1}H-NMR (300 MHz, D_2O): δ (ppm) = 4.64 (bs, 4H, –OH), 4.58 (m, 1H, H_1 or H_2), 3.73–3.30 (m, 5H, H_1 or H_2 and H_{4a}, H_{5a}), 1.94 (m, 2H, H_4 and H_5), 1.83–1.60 (m, 2H, H_3 and H_6), 1.25 (dt, J = 13.8, 5.0 Hz, 1H, H_3 or H_6), and 1.06 (q, J = 3.1 Hz, 1H, H_3 or H_6). ^{13}C-NMR (75 MHz, D_2O): δ (ppm) = 74.7, 71.0, 63.7, 59.5, 40.0, 37.1, 33.5, and 31.2. IR (KBr): 3,329, 2,928, 1,664, 1,371, 1,252, 1,033, and 513. Anal. calcd. for $C_8H_{16}O_4$: C, 54.53; H, 9.15; O, 36.32. Found: C, 54.44; H, 8.35, O, 36.71.

4.2 | Biological evaluation

4.2.1 | Biological assay for α- and β-glucosidase inhibitory activity

Inhibitory activities of the synthesized compounds were determined by conducting a spectrophotometric assay glucosidase by using PNPG (4-nitrophenyl-D-glucopyranoside), α-Glucosidase from *S. cerevisiae* (G5003; Sigma-Aldrich, St. Louis, MO) and β-glucosidase from almonds (G4511; Sigma-Aldrich) in the presence of the synthesized *rac*-cyclitol **17**, *meso*-cyclitols **18**, **19**. Acarbose was used as a positive control. Inhibitory activity was investigated according to glucosidase (α–β) inhibition assay.[32–34] Each assay was performed briefly, as follows: The reaction solution containing 1 mM PNPG (4-nitrophenyl-D-glucopyranoside) in 0.1 M natrium phosphate buffer (pH 6.8), the glucosidase (α- β-) enzyme (0.080 U/ml), and the corresponding inhibitors (the cyclitols as final structures) were incubated for 3 min at 200 rpm at 37°C. Then the reaction was stopped by the addition of 100 µl of (1 M) Na_2CO_3. After this step, the absorbances were recorded of 400 nm of the liberated *p*-nitrophenol by (Shimadzu UV-vis) spectrophotometer. The studied polyhydroxylated compounds were tested using various concentrations (10–180 µM) in buffer solution. Both synthesized compounds and acarbose (as control) were studied in triplicate.

The α- and β-glucosidases inhibition were explained (as %) as follows:

$$\text{Inhibition (\%)} = (A_{control} - A_{sample})/A_{control} \times 100.$$

4.2.2 | Test microorganisms

The pathogenic bacterial cultures chosen were *S. aureus* ATCC25923, *E. coli* ATCC1280, *S. typhi* H NCTC901.8394, *S. epidermis* ATCC12228, *M. luteus* ATCC9341, *B. cereus* RSKK-863,[19] *E. aerogenes* sp., *K. pneumonia* ATCC 27853, *P. vulgaris* RSKK 96026, *P. putida* sp., and yeast used were *C. albicans* Y-1200-NIH.

4.2.3 | Detection of antimicrobial activity

All the synthesized *rac*- and *meso*-compounds (**7**, **8**, **10**, **17**, **18**, and **19**) were examined for their antimicrobial activity by the well-diffusion method against six Gram-negative bacteria (*S. typhi* H, *E. coli*, *E. aerogenes* sp., *K. pneumoniae*, *P. vulgaris*, and *P. putida*), four

Gram-positive bacteria (*S. aureus*, *S. epidermis*, *M. luteus*, *B. cereus*), and one yeast (*C. albicans*). For the detection of antimicrobial activity, the well-diffusion method was used.[35–37]

The compounds were kept dry at room temperature and dissolved (100 and 200 µg/ml) in DMSO. DMSO was used as a solvent for the compounds and also for the control. DMSO was found to have no antimicrobial activity against any of the tested organisms. First, 1% (v/v) of 24 hr broth culture (pathogenic bacteria and yeast) containing 10^6 CFU/ml was placed in sterile Petri dishes. Then, Mueller–Hinton agar (MHA; 15 ml), kept at 45°C, was poured into the Petri dishes and allowed to solidify. Then, wells of 6 mm diameter were punched carefully using a sterile cork borer and were filled entirely with the synthesized compounds. In the last stage, the plates were incubated for 24 hr at 37°C in an incubator. On completion of the incubation period, the mean value obtained for the two wells was used to calculate the zone of growth inhibition of each sample.[19,30,31,35–39] The pathogenic bacterial cultures and yeast were tested for resistance to five antibiotics produced by Oxoid Ltd., Basingstoke, UK. These were ampicillin (prevents the growth of Gram-negative bacteria), nystatin (binds to sterols in the fungal cellular membrane and alters the permeability, allowing leakage of the cellular contents), kanamycin (used in molecular biology as an agent in isolating bacteria), sulfamethoxazole (a bacteriostatic antibacterial agent that interferes with folic acid synthesis in susceptible bacteria), and amoxycillin (a β-lactam antibiotic used to treat bacterial infections caused by sensitive microorganisms).[40–42]

4.3 | Molecular modeling studies

The crystal structure of *S. cerevisiae* α-glucosidase, in complex with its competitive inhibitor maltose, was obtained from the RCSB Protein Data Bank (PDB: 3a4a; 1.6 Å). Hydrogen atoms were added to the system with the protonate 3D tool[43] of the MOE software package (v2018.0101; Chemical Computing Group Inc., Montreal, Canada).[44] The side chains of Asn, Gln, and His were not allowed to flip during this process. Subsequently, all water molecules and the Ca^{2+} ion were omitted as they were not involved in direct binding interactions between maltose and the enzyme active site. The three-dimensional structures of *rac*- and *meso*-compounds **7**, **8**, **10**, **17**, **18**, and **19** were constructed using the MOE software package, with energy minimized using a steepest-descent protocol (MMFF94x force field) and saved as a mol 2 file before docking studies. Subsequently, the compounds were docked into the active site of the enzyme using FlexX (LeadIT, v2.3.2; BioSolveIT GmbH, St. Augustin, Germany). The active site was defined as all residues within 8 Å of the reference ligand maltose in the crystal structure active site. The highest scoring 3 poses were saved for each docked ligand for further analysis.

ACKNOWLEDGMENTS

The authors are grateful to the Scientific and Technological Research Council of Turkey (TUBITAK; Grant No. KBAG-217Z043) and the Unit of Scientific Research Projects of Sakarya University (SAU-BAP; Grant Nos. 2017-02-04-027 and 2018-01-06-153) for financial support of this study and Scientific and Technological Research Application and Sinop University Research Center of Turkey, for the use of the Bruker D8 QUEST diffractometer.

CONFLICT OF INTERESTS

The authors declare that there are no conflicts of interests.

ORCID

Arif Baran http://orcid.org/0000-0002-4117-5099

REFERENCES

[1] G. Molinari, *Pharm. Biotechnol.* **2009**, *2*, 13.
[2] a) P. B. Kaufman, L. J. Cseke, S. Warber, J. A. Duke, H. L. Brielmann, *Natural Products from Plants*, CRC Press, Boca Raton, FL **1999**; b) J. R. Hanson, *Natural Products: the Secondary Metabolites*, *Tutorial Chemistry Texts*, RSC, Cambridge, UK **2000**; c) C. Tringali, *Bioactive Compounds from Natural Compounds*, *Isolation*, *Characterisation and Biological Properties*, Taylor and Francis, New York, NY **2001**; d) J. Boik Oregon Medical Press, Princeton, MN **2001**.
[3] V. Kren, L. Martinkova, *Curr. Med. Chem.* **2001**, *8*, 1303.
[4] K. Likhitwitayawuid, B. Sritularak, *J. Nat. Prod.* **2001**, *64*, 1457.
[5] C. González, M. Carballido, L. Castedo, *J. Org. Chem.* **2003**, *682*, 248.
[6] G. Mehta, N. Mohal, S. Lakshminath, *Tetrahedron Lett.* **2000**, *41*, 3505.
[7] G. Caron, S. G. Withers, *Biochem. Biophys. Res. Commun.* **1989**, *163*, 495.
[8] G. Mehta, S. Lakshminath, P. Talukdar, *Tetrahedron Lett.* **2002**, *43*, 335.
[9] G. Mehta, R. Mohanrao, S. Katukojvala, Y. Landais, S. Sen, *Tetrahedron Lett.* **2011**, *52*, 2893.
[10] P. Gupta, A. P. J. Pal, Y. S. Reddy, Y. D. Vankar, *Eur. J. Org. Chem.* **2011**, *2011*, 1166.
[11] A. Rajender, J. P. Rao, B. V. Rao, *Tetrahedron: Asymmetry* **2011**, *22*, 1306.
[12] G. Mehta, S. Lakshminath, *Tetrahedron Lett.* **2000**, *41*, 3509.
[13] a) C. Chakraborty, V. P. Vyavahare, V. G. Puranik, D. D. Dhavale, *Tetrahedron* **2008**, *64*, 9574; b) W. Z. Gong, B. Wang, Y. L. Gu, L. Yan, L. M. Yang, J. S. Suo, *Chin. Chem. Lett.* **2005**, *16*, 747; c) B. Wang, Y. Gu, W. Gong, Y. Kang, L. Yang, J. Suo, *Tetrahedron Lett.* **2004**, *45*, 6599.
[14] S. Cantekin, A. Baran, R. Çalışkan, M. Balci, *Carbohydr. Res.* **2009**, *344*, 426.
[15] Z.-X. Guo, A. H. Haines, S. M. Pyke, S. G. Pyke, R. J. K. Taylor, *Carbohydr. Res.* **1994**, *264*, 147.
[16] H. Çavdar, O. Talaz, D. Ekinci, *Bioorg. Med. Chem. Lett.* **2012**, *22*, 7499.
[17] A. M. Gómez, E. Moreno, S. Valverde, J. C. López, *Tetrahedron Lett.* **2002**, *43*, 7863.
[18] L. Keinicke, R. Madsen, *Org. Biomol. Chem.* **2005**, *3*, 4124.
[19] S. Koçoğlu, H. Ogutcu, Z. Hayvalı, *Res. Chem. Intermed.* **2019**, *45*, 2403.
[20] A. Gypser, D. Michel, D. S. Nirschl, K. B. Sharpless, *J. Org. Chem.* **1998**, *63*, 7322.
[21] a) N. Iwasawa, T. Kato, K. Narasaka, *Chem. Lett.* **1988**, *17*, 1721; b) H. Sakurai, N. Iwasawa, K. Narasaka, *Bull. Chem. Soc. Jpn.* **1996**, *69*, 2585.
[22] S. Karadeniz, C. Y. Ataol, T. Ozen, R. Demir, H. Ogütçü, H. Bati, *J. Mol. Struct.* **2019**, *39-48*, 1175.
[23] Y. Yoshino, T. Kitazawa, M. Kamimura, K. Tatsuno, H. Yotsuyanagi, Y. Ota, *J. Infect. Chemother.* **2011**, *17*, 278.

[24] R. Martino, C. Martínez, R. Pericas, R. Salazar, C. Solá, S. Brunet, *Eur. J. Clin. Microbiol. Infect. Dis.* **1996**, *15*, 610.
[25] S. E. Kim, S. H. Park, H. B. Park, K. H. Park, S. H. Kim, S. I. Jung, J. H. Shin, H.-C. Jang, S. J. Kang, *Chonnam Med. J.* **2012**, *48*, 91.
[26] S. Dey, B. Bishayi, *Microb. Pathog.* **2017**, *105*, 307.
[27] H. Zaki, A. Belhassan, A. Aouidate, T. Lakhlifi, M. Benlyas, *J. Mol. Struct.* **2019**, *1177*, 275.
[28] R. M. Klevens, M. A. Morrison, J. Nadle, S. Petit, K. Gershman, *JAMA* **2007**, *298*, 1763.
[29] H. Öğütçü, N. K. Yetim, E. H. Özkan, O. Eren, G. Kaya, N. Sarı, A. Dişli, *Pol. J. Chem. Technol.* **2017**, *19*, 74.
[30] U. Schillinger, F. K. Lücke, *Appl. Environ. Microbiol.* **1989**, *55*, 1901.
[31] A. Altundas, Y. Erdogan, H. Ögütcü, H. E. Kizil, *Fresenius Environ. Bull.* **2016**, *12*, 5411.
[32] a) A. Baran, M. Bekarlar, G. Aydin, M. Nebioglu, E. Şahin, M. Balci, *J. Org. Chem.* **2012**, *77*, 1244; b) G. Aydin, K. Ally, F. Aktaş, E. Şahin, A. Baran, M. Balci, *Eur. J. Org. Chem.* **2014**, *2014*, 6903.
[33] a) H. Çavdar, O. Talaz, D. Ekinci, *Bioorg. Med. Chem. Lett.* **2012**, *22*, 7499; b) S. Kuno, A. Takahashi, S. Ogawa, *Carbohydr. Res.* **2013**, *8–15*, 368; c) H. Q. Dong, M. Li, F. Zhu, F. L. Liu, J. B. Huang, *Food Chem.* **2012**, *130*, 261.
[34] T. Mahapatra, S. Nanda, *Tetrahedron: Asymmetry* **2010**, *21*, 2199.
[35] C. Nithya, B. Gnanalakshmi, S. K. Pandian, *Mar. Environ. Res.* **2011**, *71*, 283.
[36] N. H. Kolhe, S. S. Jadhav, *Res. Chem. Intermed.* **2019**, *45*, 973.
[37] C. G. de Almeida, S. G. Reis, A. M. de Almeida, C. G. Diniz, *Chem. Biol. Drug Des.* **2011**, *78*, 876.
[38] S. Magaldi, S. Mata-Essayag, C. Hartung de Capriles, C. Perez, M. T. Colella, C. Olaizola, Y. Ontiveros, *Int. J. Infect. Dis.* **2004**, *8*, 39.
[39] M. Çınarlı, Ç. Y. Ataol, H. Bati, F. Güntepe, H. Ögütçü, O. Büyükgüngör, *Inorg. Chim. Acta* **2019**, *87–94*, 484.
[40] C. Valgas, S. M. Souza, E. F. A. Smânia, A. Smânia Jr., *Braz. J. Microbiol.* **2007**, *38*, 369.
[41] Y. Xiang, X. Liu, C. Mao, X. Liu, Z. Cui, X. Yang, K. W. K. Yeung, Y. Zheng, S. Wu, *Mater. Sci. Eng.* **2018**, *85*, 214.
[42] İ. Sakiyan, M. Anar, H. Oğütcü, G. Agar, N. Sarı, *Artif. Cells, Nanomed., Biotechnol.* **2013**, *42*, 199.
[43] P. Labute, *Proteins* **2008**, *75*, 187.
[44] A. Akdemir, A. Angeli, F. Göktaş, P. E. Elma, N. Karalı, C. T. Supuran, *J. Enzyme Inhib. Med. Chem.* **2019**, *34*, 528.

SUPPORTING INFORMATION

Additional supporting information may be found online in the Supporting Information section.

How to cite this article: Karakılıç E, Baran Ş, Öğütçü H, Akdemir A, Baran A. *rac*- and *meso*-Cyclohexanoids: Their α-, β-glycosidases, antibacterial, antifungal activities, and molecular docking studies. *Arch Pharm Chem Life Sci*. 2020; 353:e1900267. https://doi.org/10.1002/ardp.201900267